THE EFFECT OF AGE AND AREA OF THE BRAIN ON THE CONCENTRATION OF METALS IN Aβ PLAQUES IN TG2576 MICE

by

Erinn Gideons

A Thesis
Submitted to the
Graduate Faculty
of
George Mason University
in Partial Fulfillment of
The Requirements for the Degree
of
Master of Arts
Psychology

Committee:

Director

Department Chairperson

Dean, College of Humanities and Social Sciences

Date: July 30, 2016

Summer Semester 2010
George Mason University
Fairfax, VA

The Effect of Age and Area of the Brain on the Concentration of Metals in Aβ Plaques in Tg2576 Mice

A thesis submitted in partial fulfillment of the requirements for the degree of Master of Arts at George Mason University

By

Erinn Gideons
Bachelor of Arts
University of North Carolina-Wilmington, 2005

Director: Jane M. Flinn, professor
Department of Psychology

Summer Semester 2010
George Mason University
Fairfax, Va

DEDICATION

This Master's thesis is dedicated to my Opi.

ACKNOWLEDGEMENTS

I would to like to acknowledge all of the support from my whole family, friends and peers at GMU that I have received in this long adventure to obtaining my Master's degree. In addition I would like to acknowledge my committee, Dr. Jane Flinn, Dr. Patricia Wanschura, and Dr. Craig McDonald, for all of their assistance.

TABLE OF CONTENTS

Page

List of Tables v

List of Figures vi

Abstract vii

1. Introduction 1

2. Methods 18

Overview 18

Experimental Animals 18

Slicing 20

Microscopic Synchrotron X-ray Fluorescence: Trace Metal Detection 21

Microscopic Synchrotron X-ray Fluorescence: Multi-Channel Analysis 24

Microscopic Synchrotron X-ray Fluorescence: Peak Fitting and iImage 24

Statistical Analysis 25

3. Results 27

Overall Comparisons 27

Overall Comparisons: Individual Metal ANOVAS 30

Overall Comparisons: Cortex Differences 32

Overall Comparisons: MCA Data 33

4. Discussion 37

Conclusion 44

Appendix 1: Brain images 45

Appendix 2: Additional Tables 53

Appendix 3: Standard curve graphs for each age group 59

References.....62

LIST OF TABLES

Table Page

1. The number of mice and plaques used in the analysis.....20
2. Mean metal concentrations 28
3. The means and standard deviations of the concentrations of zinc, copper, and iron in the plaques in 12 month old mice split by sex.....53
4. Average metal concentrations in the cortical plaques across the ages.....54
5. Original Data Set.....55

LIST OF FIGURES

Figure Page

1. Diagram of the Non-Amyloidogenic and Amyloidogenic processing pathways of APP 6
2. Representative output spectrum with different element peaks and other features identified 22
3. Representative metal output images for Zn, Cu, Fe, K in one plaque 27
4. The average concentration in the plaques for each metal across the age groups....29
5. The average concentration of copper 31
6. Average concentration of the three metals in the plaques across the three age groups split into brain area....32
7. The average counts per second for each element in plaque and non-plaque brain tissue in the 18 month group 35
8. The average counts per second for each element in non-plaque brain tissue between two brain areas in the 22 month mice....36
9. Region of Interest 1: Interaural .64, Bregma -3.16 45
10. Region of Interest 2: Interaural 1.74, Bregma -2.0 46
11. Region of Interest 3: Interaural 2.34, Bregma -1.46 47
12. Region of Interest 4: Interaural 3.1, Bregma -.70 48
13. Region of Interest 5: Interaural 4.54, Bregma .74 49
14. Representative brain slice from a 12 month old Tg2576 mouse 50
15. Representative brain slice from a 18 month old Tg2576 mouse 51
16. Representative brain slice from a 22 month old Tg2576 mouse 52
17. Standard curve graphs for sheep brain standards for the 12 month group mice....59
18. Standard curve graphs for sheep brain standards for the 18 month group mice....60
19. Standard curve graphs for sheep brain standards for the 22 month group mice....61

ABSTRACT

THE EFFECT OF AGE AND AREA OF THE BRAIN ON THE CONCENTRATION OF METALS IN Aβ PLAQUES IN TG2576 MICE

Erinn S. Gideons

George Mason University, 2010

Thesis Director: Dr. Jane M. Flinn

Studies have shown increased amounts of essential trace metals, zinc, copper, and iron, in human brains afflicted with Alzheimer's disease (AD) and brains of transgenic mouse models of AD. However, no reports have been published on the concentrations in the amyloid plaques of an AD mouse model or the change in trace metal deposition in amyloid-β plaques with age. This study examined the change in concentrations of trace metals that occur with increasing age in the amyloid-β plaques in the brains of Tg2576 mice, a murine model of Alzheimer's disease. Microprobe synchrotron x-ray fluorescence (SXRF), a non-destructive technique that can measure all of the elements present in the tissue at one time was used in this study. Additionally, comparisons were also done on the concentrations of zinc, copper, and iron across the three ages in the cortical plaques. Finally, differences in the counts of zinc, copper, iron, potassium, and calcium between plaque tissue and non-plaque brain tissue were investigated.

The results showed a significantly lower concentration of copper in the plaques of the cortex of the oldest age group, 22 months, compared to the youngest group of mice, 12 months. There was also an overall trend towards significantly more copper in the cortical plaques compared to the hippocampal plaques. Finally, multi-channel analyses (MCA) showed that there were significantly higher counts of zinc, copper, iron, and a strong trend toward higher counts of potassium in the plaque tissue compared to the non-plaque brain tissue in the 18 month age group.

Introduction

Alzheimer's disease (AD) is the most common form of dementia. It was first described as a distinct form of dementia by Alois Alzheimer in 1906. AD is characterized by progressive memory loss, cognitive impairment, and behavioral changes. These outward symptoms are mirrored by pathological symptoms that include neuronal and axonal degeneration, amyloid plaques, and neurofibrillary tangles (NFTs) along with additional changes at the cellular and molecular level. Amyloid plaques consist primarily of the amyloid-beta (Aβ) protein of two different lengths of either 40 or 42 amino acids, which are cleaved from the transmembrane amyloid precursor protein (APP). Alzheimer's disease has been diagnosed in people as early as 30 years of age, but usually occurs in people 60 years and older. Alzheimer's disease diagnosed from 30-60 years of age is usually termed early onset, while late onset AD is the diagnosis given to people 65 years and older. There are no symptomatic differences between the two forms of the disease (Bayer et al., 2001). In a majority of late onset cases, AD is thought to have idiopathic origins, meaning that there is no clear cause, whether genetic or environmental; these cases are called sporadic AD. However, a majority of early onset AD cases have been found to be caused by a variety of genetic mutations and are known as Familial AD. Although there are no genetic mutations currently known that cause late

onset AD, a polymorphism of apolipoprotein E (APOE), APOE4, is a well-established risk factor.

Interestingly, trace metals, zinc (Zn), copper (Cu), and Iron (Fe), which are necessary for normal brain functioning and found in relatively high levels in brain tissue, are found in higher concentrations in AD brains. The high concentrations are seen in plaques and the surrounding brain tissue (Lovell, Robertson, Teesdale, Campbell, & Markesberry, 1998). A variety of methods have been used to detect, localize, and measure amounts of Zn, Cu, and Fe in AD brains. One of these techniques includes inductively-coupled plasma- mass spectrometry (ICP-MS), which completely destroys the tissue to measure total amounts of all detectable elements (Diebel, Ehmann, & Markesberry, 1996). In addition, the many histological stains that have been used to visualize the location of these metals, such as the Prussian Blue stain which stains for iron and immunocytochemical methods, can wash away metals or introduce unwanted artifacts into the tissue (Sayre et al., 2000). By using microscopic synchrotron X-ray fluorescence (SXRF), it is possible to measure the concentration and location of various elements present in the tissue without washing away any unbound metals or harming the tissue. Because use of SXRF techniques is relatively new to the biological sciences, there have been limited studies with this technology to determine if the concentration of Zn, Cu, and Fe increase with age in senile plaques and surrounding parenchyma of Tg2576 mice, a transgenic murine model of AD.

The brains of Alzheimer's disease sufferers have high levels of extracellular plaques and intracellular tangles when autopsied, along with other indicators of extensive damage caused by the disease, such as neuronal loss and oxidative stress. Alzheimer's disease progresses through the brain in a regular pattern in most cases. Braak and Braak (1991) performed autopsies on 83 demented and non-demented brains to delineate the course of AD pathology through the brain. In the early stages of the disease, neurofibrillary tangles begin to appear in the hippocampus and entorhinal cortex in the temporal lobe. In addition, amyloid deposits are present in the basal areas of the frontal, temporal and occipital lobes of the neocortex. The hippocampus has three main subfields, CA1 (cornu ammonis), CA3, and the dentate gyrus. It is associated with both episodic memory and spatial memory (Squire, 1992). Semantic memory is stored in the temporal lobe, mainly in the entorhinal cortex. The frontal cortex is involved with planning, organization, and sequencing of memories, source memory, working memory, and inhibition of emotional responses initiated by the amygdala (Chayer & Freedman, 2007). As the disease advances, more of the hippocampus and surrounding cortex become inundated with NFTs. In addition, amyloid deposits are seen throughout the neocortical association areas. The neocortical association areas are involved with a variety of functions, including language and body perception. However, the hippocampus does not yet contain high levels of amyloid deposition. In the end stages of AD, most of the brain is littered with both NFTs and amyloid deposits. The motor cortices are the last areas affected by Alzheimer's disease. The progression of behavioral, personality, and memory changes is not as well delineated, but generally

mirrors the deconstruction of the brain. In 2004, Klunk et al. published the first report of imaging amyloid with positron emission tomography (PET) in living human patients diagnosed with AD and control subjects. This novel technique allows researchers and physicians to measure relative concentration of amyloid in the brain and trace the progression of plaques in living patients rather than relying on post-mortem brains.

Senile plaques are a hallmark of Alzheimer's disease. They are composed primarily of the amyloid-beta (Aβ) peptide. The structure of Aβ was isolated and sequenced from samples of deposits of amyloid around blood vessels in the brain, called cerebral amyloid angiopathy (CAA) by Glenner and Wong in the early 1980s (Glenner & Wong, 1984). It was later discovered that Aβ is cut from a larger protein named amyloid precursor protein (APP), whose coding sequence is located on chromosome 21 (Tanzi et al., 1987). APP is a large transmembrane protein ranging from 695-770 amino acids in length and is found ubiquitously throughout the body; APP 695 is most likely to be found in neuronal cells (Selkoe, 1998). Although the function of APP is unclear, it is thought to be involved in synaptogenesis, synaptic plasticity, and metal ion homeostasis (Smith, Cappai & Barnham, 2007). APP has a large amino (N)- terminal extracellular domain, one transmembrane domain, and a small cytoplasmic domain (Beher, Hesse, Masters, & Multhaup, 1996). It also has metal binding sites for both copper and zinc in the N-terminal domain and the Aβ domain, and a high binding affinity to iron (Adlard & Bush, 2006). APP can be catalyzed by three different secretases, alpha (α), beta (β), and gamma (γ). Most of the time, especially in non-neuronal cells, α-secretase cuts APP in the middle of the Aβ sequence, which releases the soluble extracellular APP domain and

leaves the rest of APP attached to the cell membrane. Then γ-secretase cleaves the intact APP which produces the APP intracellular domain and the p3 fragment (Evin & Weidemann, 2002). This processing of APP is known as the "non-amyloidogenic pathway" because it does not produce Aβ. In contrast, amyloid β is produced when APP undergoes consecutive cleavages by β-secretase and γ-secretase; this is called the "amyloidogenic pathway". The cleavage by β-secretase releases a shorter soluble APP extracellular domain and then γ-secretase cuts the intact APP within the hydrophobic transmembrane domain producing Aβ and the APP intracellular domain. Depending on where γ-secretase cuts, Aβ can be between 39-43 bases long. Refer to Figure 1 for a diagram of the two APP processing pathways (Sambamurti, Hardy, Refulo, & Lahiri 2002). $A\beta_{1\text{-}40}$ is the most common Aβ peptide produced by the amyloidogenic pathway; $A\beta_{1\text{-}42}$ is the second most common. The longer Aβ peptides are far less soluble (sAPP) than the shorter peptides. Additionally, $A\beta_{1\text{-}42}$ is the only Aβ peptide known to have the ability to form oligomers *in vivo* (Haass & Selkoe, 2007).

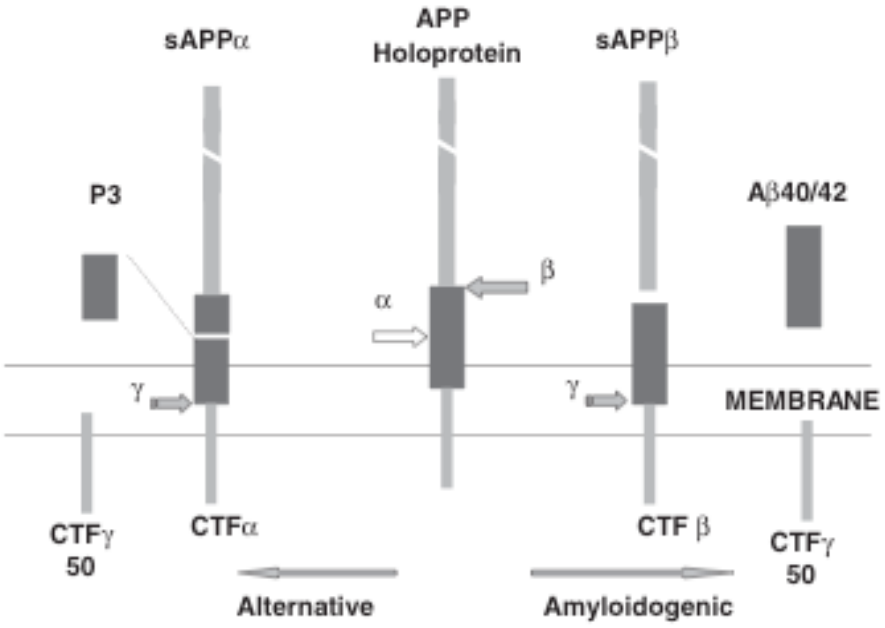

Figure 1. Diagram of the Non-Amyloidogenic and Amyloidogenic processing pathways of APP. CTF: C-terminal fragment of APP. P3: smaller fragment of Aβ when cleaved by α-secretase.

After cleavage from APP in the amyloidogenic pathway, hydrophobic Aβ peptides of varying numbers of amino acids are released into the extracellular space and in internal membranes of cells (Haass & Selkoe, 2007). The length of the peptide influences its ability to aggregate into oligomers, with the longer peptides having the greatest potential for aggregation. $A\beta_{1\text{-}42}$ forms oligomers that progress into soluble non-fibrillar plaques. Eventually soluble plaques form non-soluble plaques that begin to acquire more fibrils of different Aβ lengths (Haass & Selkoe, 2007). Insoluble plaques can also be formed when soluble oligomers come into contact with other macromolecules and cell walls. The formation of Aβ aggregates is assisted by interaction with the

transition metals, zinc, copper and iron. Kuo et al. (1996) found soluble Aβ levels were six times higher in AD brains compared to non-demented brains. Additionally, insoluble Aβ levels were at least 100 times higher in AD brains than in control brains. Some researchers have hypothesized that soluble Aβ oligomers are more destructive than non-soluble plaques because the amount of soluble oligomers measured through western blotting and Aβ enzyme-linked-immunosorbent assays (ELISAs) associate better with cognitive deficits than senile plaque counts (Lue et al., 1999; Naslund et al, 2000). In addition, soluble oligomers can diffuse into the synaptic cleft, which can cause significant synaptic dysfunction. In contrast to previous research that soluble Aβ alone was toxic, Opazo et al (2002) found that Aβ is not toxic without the presence of Cu^{2+}, Fe^{3+}, or Zn^{2+}.

Senile plaques are sphere-like deposits about 50-200 μm in diameter with a core loaded with $A\beta_{1-42}$. At later disease stages, the plaques transition to have more $A\beta_{1-40}$ at their core. Dystrophic neurites and other evidence of astrocyte and microglia activation surround them. Late stage senile plaques bind with Congo Red and Thioflavin-S dyes, which are attracted to the cross-β-pleated sheets of the plaques. Some researchers believe that senile plaques are the entombment of pathogenic soluble Aβ (Haass & Selkoe, 2007). However, dense core plaques have been shown to be harmful to surrounding tissue as well, as evidenced by synaptic damage surrounding the insoluble plaques (Tsai, Grutzendler, Duff, & Gan, 2004). Plaques form in the brain parenchyma and in the cerebral blood vessels.

Early onset Alzheimer's disease is AD that is diagnosed between 30-60 years of age. Most cases of early onset AD follow a genetic inheritance pattern, either a combination of genetic factors or an autosomal dominant pattern. The pathogenic mutations are found in the following genes: Presenilin 1 (PS1), Presenilin 2 (PS2) and Amyloid Precursor Protein (APP), on chromosomes 14, 1, and 21, respectively. These mutations account for more than 50% of familial AD cases, with mutations in PS1, which is part of the γ secretase, predominating (Newman, Musgrave, and Lardelli, 2007). Amyloid Precursor Protein contains the sequence for amyloid β peptide. The APP mutations are generally located near the cleavage sites of β- and γ-secretase. The APP mutations within the Aβ sequence directly affect the folding of the Aβ peptide (Haass & Selkoe, 2007). Amyloid Precursor Protein mutations cause about 8-16% of familial AD cases (Raux et al, 2005). Presenilin 1 has multiple biological functions, including cellular transport, signaling pathways, and apoptosis (Kowalska, 2004). PS1 is part of the gamma-secretase complex, which is comprised of four membrane proteins and cleaves APP and Notch (Chapman, Falinska, Knevett, & Ramsay, 2001; Newman et al., 2007). As part of the gamma-secretase complex, PS1 is located in the membranes of the golgi apparatus and the endoplasmic reticulum of cells. Multiple researchers have discovered that PS1 mutations affect APP processing and cause an increase in the overall production of Aβ42 peptides (Scheuner, et al., 1996; Shen & Kelleher, 2007; de Strooper, et al., 1998). There are only 10 known PS2 mutations affecting six families with familial Alzheimer's disease. In comparison with PS1, relatively little is known about Presenilin 2's functions. Overall, PS1 and PS2 mutations are involved in about 80% of familial AD

cases (Raux et al., 2005). Late onset Alzheimer's disease, unlike early onset Alzheimer's disease, has no known genetic causes. However, isoforms of apolipoprotein E (APOE) mediate a "dose dependent" risk factor for late onset AD (Chai, 2007). It is important to note however that APOE is neither necessary nor sufficient to cause AD.

Following the identification of causal genetic mutations for Alzheimer's disease, the development of transgenic animal models of the disease became a new area of research. Animal models have allowed researchers to study many aspects of Alzheimer's disease that are not possible to delineate in humans and have led to many discoveries about the molecular, cellular, and pathological changes seen in AD brains (Newman et al., 2007). Additionally clinical trials of possible treatments and biomarkers are usually performed on transgenic animals before moving to humans. There are a variety of methods to develop mouse models of AD, including overexpressing mutations of human genes APP, PS1, PS2, tau, APOE and selected crossing of these mutations. Each mouse line develops some Alzheimer's disease-like characteristics, although no model shows all the behavioral, biochemical, and pathological features seen in human AD brains. One of the first and most well characterized transgenic AD mice developed is the Tg2576 line. The Tg2576 mice overexpress human APP containing the Swedish mutation, a double mutation at the 670 and 671 amino acids, Lysine -> Asparagine, Methionine -> Leucine respectively, with a hamster prion protein promoter (Hsiao et al., 1996). The level of human APP overexpression is approximately fives times more than that of endogenous mouse APP (Janus, Chisthi, & Westaway, 2000). Memory deficits begin around 9 months of age or slightly earlier, depending on the task (Ashe, 2001). Specifically, Tg2576 mice

display impaired spatial learning assessed by the Morris Water Maze, decreased spontaneous alternation in the Y-maze paradigm, and impaired spatial working memory assessed by the forced choice T-maze alternation test (Hsiao et al., 1996). Tg2576 mice also have deficits in the cued and contextual fear conditioning paradigms (Kobayashi & Chen, 2005). These memory deficits get progressively worse over time. Additionally, hippocampal neurons display reduced long-term potentiation around the time of plaque deposition and following plaque deposition (Chapman et al., 1999). Long-term potentiation is believed to be one of the cellular mechanisms underlying learning and memory. Behavioral studies in Tg2576 mice have provided strong evidence that insoluble Aβ plaques disrupt cognition.

The human homologue of APP must be overexpressed because mouse APP, which does not bind zinc, copper, and iron as strongly as human APP, does not form plaques. Chelation of zinc ions, copper ions, and iron ions by APP can induce histidine-bridging between Aβ molecules resulting in the formation of Aβ plaques. Rat and mouse Aβ peptides have an arginine residue substituted for the bridging histidine residue; therefore amyloid aggregation is less likely to occur (The UniProt Consortium, 2010). Amyloid-β plaques can first be seen in Tg2576 mice at approximately 9 months of age. The plaques can most easily be found in the hippocampus, cerebral cortex and amygdala; they are also seen in other brain structures. The plaques can be stained with Congo Red, which identifies the β-pleated sheet protein structure in the amyloid plaques under bi-refringence. In addition, there is evidence of astrocytosis, microgliosis, and some hyperphosphorylated tau in the brains of Tg2576 mice (Chapman et al., 1999; Hsiao et

al., 1996). Notably, there is no apparent neuronal loss or neurofibrilliary tangles, which are pathological hallmarks of human AD.

Zinc, copper, and iron are trace elements essential for development and proper functioning of the brain. These elements are known as transition metals because of their position on the periodic table. Iron and copper can occupy multiple valence states and are redox active. In general, transition metals can form ions with a multitude of oxidation states and are good catalysts (Adlard & Bush, 2006). Copper and iron can be present in two stable oxidation states *in vivo;* copper as Cu^{1+} (cuprous) or Cu^{2+} (cupric), and iron as Fe^{2+} (ferrous) or Fe^{3+} (ferric). Each metal is found in relatively high levels in the brain at autopsy. Also, their homeostasis in cells and in the body is tightly regulated by a myriad of factors, including multiple metal storage and transport proteins. The blood brain barrier controls their transport into the brain.

In comparison with other organs, the brain has the highest amount of zinc in the body (Mocchegiani, Berton-Freddari, Marcellini, & Malavolta, 2005). Zinc has been found in more than 200 enzymes, helps stabilize many proteins' structure, and seems to prevent the formation of free radicals (McCall, Huang, & Fierke, 2000). Histological staining of brains unaffected by AD has revealed that the hippocampus, amygdala, and parietal lobe are the areas with the highest amounts of zinc, which are also areas inundated with plaques and tangles in end-stage AD (Frederickson, Koh, & Bush, 2005). A high percentage of zinc is bound to proteins while unbound zinc is mostly found in presynaptic vesicles in grey matter.

The highest concentrations of copper are found around the synaptic clefts of glutaminergic and adrenergic neurons in the hippocampus, olfactory bulb, and locus coeruleus (Mathie, Sutton, Clarke, & Veale, 2005). Copper is also involved in myelination. After neuronal depolarization, zinc and copper are released and can be found in pools around the synaptic cleft.

Iron is bound to the protein transferrin and constantly transported throughout the brain in the blood. It can also be found bound to other molecules, like ferritin, citrate, adenosine triphosphate (ATP), and ascorbic acid (Moos, Rosengren, Skjorringe, & Morgan, 2007). Iron is released from both neurons and oligodendrocytes into the extracellular space of the brain, where it can come into contact with a variety of brain structures. The highest concentrations of iron are found in the basal ganglia in the adult human brain (Hill, 1998).

Multiple studies on humans and rodents, both rats and mice, have shown copper and iron amounts in the brain increase significantly throughout life, while zinc levels generally do not increase (Adlard & Bush, 2006). However, Lee et al. (2002) found that total zinc in the brain does increase in female Tg2576 mice with age but not in male Tg2576 mice. Many studies have found an imbalance of zinc, copper, and iron in demented brains. Lovell et al. (1998) found that all three metals showed a three to five fold increase, specifically in the cortical and basal nuclei of the amygdala of human AD brains, compared to age-matched controls. Additionally, zinc (1055 μM), copper (390 μM), and iron (940 μM) levels were significantly increased within the Aβ plaques when

compared to the neuropil of age-matched controls, zinc (350 μM), copper (70 μM), and iron (340 μM) (Lovell et al., 1998). Because of these differences, a lot of research has been focused on identifying the relationship of zinc, copper, and iron with the pathogenesis of AD, and more specifically their relationship with APP and Aβ. The APP sequence, including the sequence coding for Aβ, have histidine-mediated metal binding sites for copper and zinc. Also, an iron regulatory element affects the translation of APP; translation of APP is up-regulated by iron exposure (Adlard & Bush, 2006). Consequently, it has been found that changing copper levels *in vitro* can regulate APP mRNA expression, and therefore have an effect on Aβ production. In an acidic environment, copper causes Aβ to form insoluble plaques (Atwood et al., 1998). Additionally, zinc causes secreted APP and Aβ to form aggregates at a physiological pH (7.4) *in vitro* (Brown et al., 1997). Genetic deletion of the zinc transport protein, zinc transporter -3 (ZnT3), in Tg2576 mice causes a significant reduction in the amount of plaques in the brain (Lee et al., 2002). It has been found that overexpression of the Swedish APP mutation in a mouse, the Tg2576 mouse, resulted in elevated zinc in the plaques found in the brain (Lee et al., 1999). A study investigating the location of increased iron in relation to Aβ plaques in PS/APP mice, a mouse model with overexpression of both human PS1 and human APP, found that increased staining for iron was colocalized with Aβ plaques (Falangola, Lee, Nixon, Duff, & Helpern, 2005). Iron levels were increased but lower copper levels were found in Tg 2576 compared to non-transgenic littermates (Maynard et al., 2002; Smith et al., 1998). However, dietary copper supplementation in APP23 mice, another Swedish mutation AD model, resulted in

lower amounts of soluble $A\beta_{1-40}$ and $A\beta_{1-42}$ levels in the brains of male mice (Bayer et al., 2001). It is possible that the presence of additional copper shifted amyloidogenic processing of APP to the non-amyloidogenic pathway (Borchardt et al., 1999). These studies and many others show that metal ion dishomeostasis can significantly affect APP processing, amyloid processing and plaque deposition in AD mouse models.

In addition to having an effect on amyloid, copper, and iron also play an important role in oxidative stress, another hallmark of AD pathology. Evidence of increased oxidative damage, elevated levels of reactive oxygen species (ROS) and higher amounts of oxidated proteins, is seen in AD brains. Plaque deposition is preceded by oxidative stress damage to neurons (Nunomura et al., 2001). When oxygen is reduced, ROS such as hydrogen peroxide and hydroxyl radicals are produced (Adlard & Bush, 2006). Reactive oxygen species in cells are mostly made from the interaction of oxygen with redox-active metals, copper and iron. Although a small amount of ROS is helpful for the cell, huge increases in ROS production can cause lipid peroxidation, enzyme inactivation, and changes protein structure. The body does have natural defense mechanisms to ROS production called anti-oxidants. However, there is evidence of decreased anti-oxidant levels in AD brains. Additionally, Aβ interaction with copper and iron causes chemical reduction of both metal ions (Cu^{2+} to Cu^{1+} and Fe^{3+} to Fe^{2+}) which produces hydrogen peroxide with the addition of oxygen (Bush, 2003). When the reduction of Cu is not in combination with another substrate, oxidation of Aβ side chains occurs, which leads to oligomerization (Bush, 2008). After hydrogen peroxide is produced, it is then reduced through a Fenton Reaction into the more reactive hydroxyl

radical. Therefore the generation of ROS plays a role in the toxicity of Aβ. Huang et al. (1999) found that toxicity of Aβ-Cu^{2+}/Fe^{3+} is related to Aβ peptide length, with the $A\beta_{1-42}$ combination being the most toxic.

Microprobe Synchrotron X-ray Fluorescence (SXRF) technology is an excellent way to measure trace element composition of biological materials. In SXRF analysis, high energy X-rays in the form of synchrotron light irradiate a point on the tissue and cause electrons to move to higher energy shells of the atoms in the sample. When the vacancies on the lower shells are refilled, characteristic X-rays for each element present are emitted, then detected, and used for quantitative analyses of elements in the tissue at that point (Jones et al., 1988). The use of synchrotron light in the x-ray range allows for high spatial resolution because of its short wave lengths and high intensity. The light can be focused into spot sizes in the 2-10 μm range. It also has extremely sensitive element detection, in the sub mg kg^{-1} (sub-parts per million) range (Miller et al., 2005). Therefore, trace elements can be measured *in situ*. Additionally XSRF is non-destructive to the tissue because of the low power deposition of X-rays and the ability to conduct the analyses in air (Miller et al., 2005). Also, because the tissue does not need to be fixed or stained before SXRF data collection, there is little possibility for sample contamination or the elements being washed off the tissue..

In addition to traditional SXRF data collection on a square area surrounding a plaque or other area of tissue, another technique, multi-channel analysis (MCA), is done using the synchrotron x-ray. During MCA data collection, the X-ray beam is fixed on

point in the tissue for five minutes, instead of seven seconds per pixel in the maps of the plaques. Multi-channel analysis is done because it allows for a more complete picture of the elemental makeup of the spot where the beam is focused. The X27A beamline at the National Synchrotron Light Source (NSLS) at Brookhaven National Laboratory is able to detect a variety of elements, including potassium, calcium, iron, copper, nickel and zinc.

The main purpose of this study is to determine the time course of trace metal deposition in plaques and surrounding parenchyma in a mouse model of Alzheimer's disease. A secondary goal is to ascertain if there are different concentrations of zinc, copper, and iron in two different brain regions, the hippocampus and the cortex in the Tg2576 mouse. In addition, MCA data will be used to look at elemental differences in plaque and non-plaque brain tissue in the AD mouse model. My hypothesis is the concentration of zinc will not change significantly with age. I hypothesize that the concentration of iron will increase significantly in the plaques as the animals age. I hypothesize the increase in iron will occur because as the mice age and levels of oxidative stress increase, more iron will be pulled into the redox reaction with amyloid β. I also hypothesize that the concentration of copper will not increase significantly in the plaque tissue; it will show a decrease from the 12 month group to the 22 month group. It has been shown that copper amounts are lower in the Tg2576 brains after the appearance of amyloid plaques (Maynard et al., 2002) and APP knockout mice have an increase in brain copper levels (White et al., 1999). However, the concentration of copper will decrease with as the mice age because the ratio of Aβ1-40/Aβ1-42 increases with time and copper is not as tightly bound to Aβ1-40. In respect to the brain area analysis, I

hypothesize that the plaques in the cortex will have a higher concentration of all of the metals. Lastly, I hypothesize that there will be higher counts of each metal in the plaques compared to the non-plaque brain tissue because of previous research on human AD brains and Tg2576 mice brains. I hypothesize there will be no significant differences in the counts of each element between the cortex and hippocampus. The analyses were done with XSRF technology to measure zinc, copper, and iron and other elements in unfixed tissue, therefore it is less likely the slices were contaminated or histopathological stains and buffers affected the metals in the tissue. Brain slices from Tg2576 mice culled at three different ages, 12 months, 18 months, and 22 months, were examined at beamline X27A at NSLS at Brookhaven National Laboratory. Then statistical analyses were performed to examine any differences in the concentration of metals at the three different ages.

Methods

Overview

This experiment consisted of three cohorts of transgenic (Tg) APP2576 mice sacrificed at different ages, 12, 18, and 22 months, which are called Cohorts 3, 4, and 5 respectively. The cohorts also include wild type (Wt) mice but they were not analyzed, as their brains do not contain amyloid plaques. A subset of the Tg mice from each cohort, which drank water with no additional metals was selected to be analyzed. Microscopic synchrotron X-ray fluorescence (SXRF) was used to detect trace amounts of zinc, copper, and iron in amyloid plaques and surrounding tissue in brain tissue from the mice. Synchrotron X-ray fluorescence was also used to perform MCA data collection on individual points in either plaques or non-plaque brain tissue for the 18 month group and only non-plaque brain tissue in the 22 month group to collect data on all elements present.

Experimental Animals

The three cohorts of APP2576 mice were raised at George Mason University (GMU). The 12 month mice were bred at GMU. The 18 month and 22 month mice were purchased from Taconic (New York) at 12 weeks of age. They had access to food and water *ad libitum*. They were group housed with access to Nyla bones and running

wheels, and were kept on a 12 hr light/dark cycle. In Cohort 3 there were nine Tg mice (n=5 male; n=4 female) on tap water. They were sacrificed at 12 months of age. Cohort 4 consisted of 9 Tg mice but analysis was only done on 5 animals; their brains were extracted at approximately 18 months. Cohort 5 mice were mice from Cohort 4 that were not sacrificed at 18 months; they were sacrificed at 22 months instead of 24 months because they were dying of various health complications. There were 10 Tg mice on tap water (all females). Additionally Cohort 5 animals were either injected with Feralax (a metal chelator) or a control (Ringer's solution). Only control animals, i.e. injected with the Ringer's solution, from Cohort 5 was used in the analysis. Only females were purchased for Cohort 4 because the male mice fought extensively and therefore had to be singly housed. To maximize cage space the decision was made to only use female mice for further experiments. In Cohorts 3 and 4 there were also groups of mice that drank water spiked with iron, zinc, or zinc plus copper. These mice were not used in the analyses. See Table 1 for a break down of the number of animals from each cohort and the number of plaques analyzed from each cohort.

Table 1. The number of mice and plaques used in the analysis.

Age	Number of mice	Number of plaques
12 months	9	15
18 months	5	16
22 months	9	34

Slicing

Brains were extracted from sacrificed mice and immediately flash-frozen on dry ice and stored at -80^{o}C. Coronal slices for XSRF investigation and Congo Red staining were sliced consecutively at 20 μm. XSRF slices were mounted on pure silica slides to reduce the chance of contamination. Each animal had one XSRF slide and one adjacent Congo Red slide that contained slices for five regions of interest (ROI): 1-ventral hippocampus (Interaural .64 mm, Bregma -3.16mm), 2-dorsal hippocampus (Interaural 1.74 mm, Bregma -2.06 mm), 3- anterior-dorsal hippocampus (Interaural 2.34 mm, Bregma -1.46 mm), 4- basal ganglia (including the amygdala) 1 (Interaural 3.10 mm, Bregma -.70 mm), 5-basal ganglia (including the amygdala) 2 (Interaural 4.54 mm, Bregma 0.74 mm). See figures A1-A5 in the Appendix for images of the regions of

interest 1-5, respectively. Additional slices were taken for other analyses and stored at -80^{o}C. Leftover brain tissues were also stored at -80^{o}C.

Microscopic Synchrotron X-ray Fluorescence: Trace Metal Detection

All X-ray analysis was done on beamline X27A at the National Synchrotron Light Source (NSLS) at Brookhaven National Laboratory (BNL), Upton, NY USA. The beamline was tuned to 12 KeV using a Si(311) monochromator. The original 1mm x 1mm beam was focused to 0.015 mm (h) x 0.010 mm (v) using two rhodium coated silicon mirrors placed using Kirkpatrick-Baez geometry. The beam has an average flux of $5x10^{9}$ ph/sec. The working distance between the sample and the detector was 9 cm. For two-dimensional composition mapping, counting times of 7 sec/pixel were used, with step sizes of 10μm between each point. Using a plotting program written by researchers at NSLS, a rectangle map was made around each plaque or area of interest that instructed the beam where to collect counts. At each 10 μm step, fluorescence counts for all elements in the tissue of interest, including but not limited to zinc, copper, iron, potassium, and calcium, were extracted from the X-ray spectra. The program also produced a raster color image for each element chosen for each map. The areas of the metals and other elements in the spectra were determined by choosing regions from the X-ray emission lines by focusing the beam on tissue for three minutes and then manually setting the peak region of interest in the plotting program. See Figure 2 for a representative spectrum with different element peaks identified.

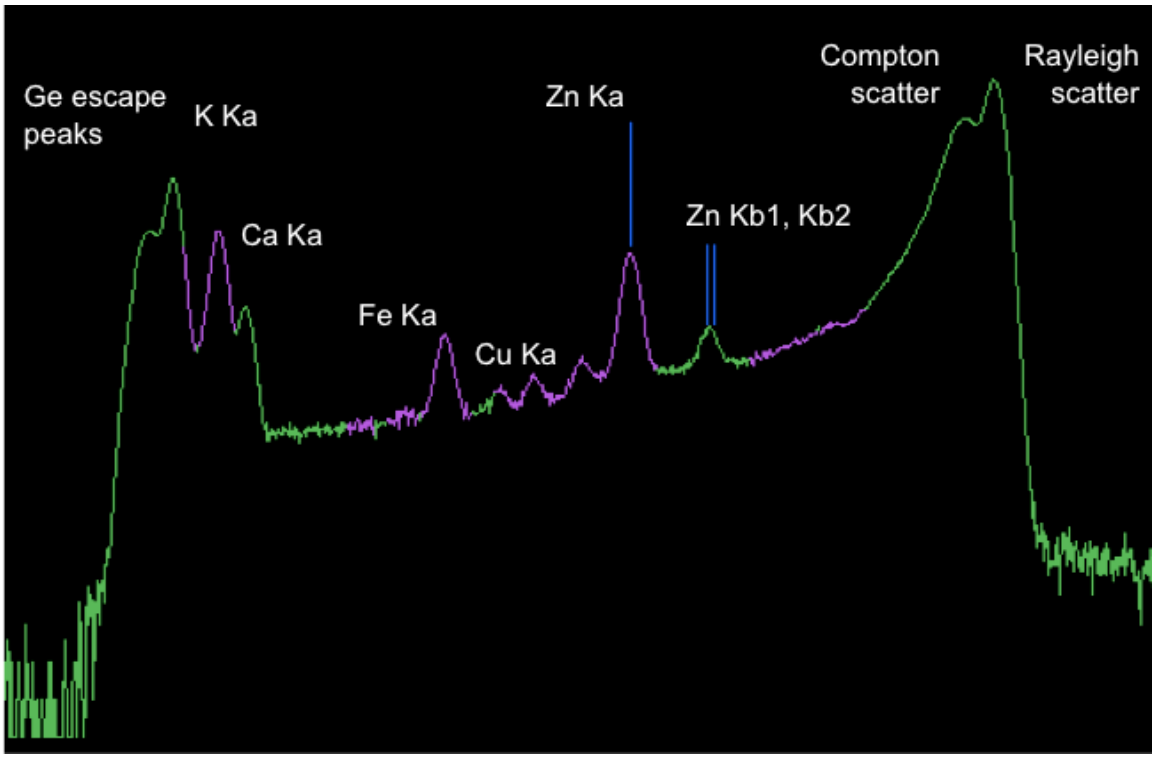

Figure 2. Representative output spectrum with different element peaks and other features identified. A representative spectrum from one plaque with different element peaks in purple. Other features of the spectrum are also identified. Ka: first X-ray energy emission line. Kb: second X-ray energy emission line

The output is calculated in counts per second by dividing the total counts for the area under the peak for that element by the total number of seconds it took for the map. The data was collected over multiple collection times, which necessitated a method to standardize the counts because the SXRF beam changes from run to run. Homogenized cortex from sheep brain was spiked with pre-determined concentrations of different elements and lab water as a control, frozen, and then sliced at 20 μM on pure silica slides. During data collection, 10 μM x 10 μM areas from each element concentration were also

run on the SXRF. The counts for the different concentrations of the different elements were used to make a standard curve. The equation of the standard curve for each element was used to convert the counts collected into parts per million (ppm) concentrations for each plaque. It was impossible to make potassium standards because of the naturally high levels of potassium in the sheep brain.

Microscopic Synchrotron X-ray Fluorescence: Multi-Channel Analysis

After running the maps of the plaques of interest, the area with the highest concentration of zinc, copper, and iron within each plaque was chosen to run a MCA for the 18 month mice. Also, a spot in the brain area near the plaque was also chosen to collect data for non-plaque values for both the 18 month and 22 month mice. MCAs were not run on the 12 month mice brain tissue and were not run on plaque tissue in the 22 month mice because of a lack of time while doing data collection. The x-ray beam is tuned in the same way as for map data collection, but instead of the beam moving after 7 seconds, it is focused on the same spot for 5 minutes. The output is also calculated in counts per second by dividing the total counts by the total number of seconds. Because no standards were collected using the MCA method, it was not possible to standardize the counts into parts per million. Additionally, there was one outlier in the counts for calcium in the 18 month group; it was replaced with the 18 month average count for calcium since none of the other element counts were outliers.

Microscopic Synchrotron X-ray Fluorescence: Peak Fitting and iImage

A program, Peak Fit, was made to account for human error in selection of the

total peak of energy for each element at the beginning of data collection runs. In the data-plotting program, the area of interest is circled and the energy peaks for each pixel circled are summed and transferred to the Peak Fit program. First, a background line for the spectrum must be identified. Then the known elemental and other energy peaks are identified in the spectrum, the characteristic energies are inserted, and they are listed in the Peak Fit program output. Once all the peaks have been identified and the Peak Fit spectrum matches the experimental spectrum, the original peaks are modified to the Peak Fit peaks. To obtain the values from the images produced by the data-plotting program, the iImage program was used. The Peak Fit images are opened in iImage for each element of interest individually. The area of interest, the plaques in this study, is then circled and the values of each pixel in that area are averaged to produce the mean value of each element for that area.

Statistical Analysis

To assess whether there were significant differences in the concentrations of zinc, copper, and iron in the plaques of the 12 month, 18 month, and 22 month mice a repeated measures analysis of variance (RMANOVA) was performed. Then individual 3x2 analyses of variance (ANOVA) were independently run for zinc, copper, and iron with age (12 months, 18 months, and 22 months) and brain area (hippocampus and cortex) as the independent variables. The brain areas were also split and individual ANOVAs were run for each metal to check for changes in the concentration of the metals with age in the individual brain areas. Additional ANOVAs were performed to check for significant

differences in the amount of each metal in the males and females in the 12 month group to determine if the two sexes could be combined into one group for further analysis. Sine there were no significant gender differences, zinc ($F(1,14) = 2.70$, $p > .05$), copper ($F(1,14) = 3.81$, $p > .05$), iron ($F(1,14) = .503$, $p > .05$), the male and female data was combined for all the analyses. Analysis of variance tests were performed on the MCA data to check for differences in the counts of zinc, copper, iron, potassium, and calcium in the type of tissue (plaque versus non-plaque) and brain area (hippocampus versus cortex) in the 18 month mice. Analysis of variance tests were performed on the MCA data to check for differences in the counts of zinc, copper, iron, potassium, and calcium in the brain areas (hippocampus versus cortex) in the 22 month mice. Originally, plaques from a third brain area, the basal ganglia, were going to be analyzed, however data for only six basal ganglia plaques was collected which resulted in highly unequal group numbers so they were omitted. There were two zinc values that were outliers in the 12 month age group, which is defined as values more than two standard deviations away from the mean. Those outlier values were changed to the mean value of zinc in the 12 month age group for the analysis. There was also one outlier in the 18 month MCA data in the calcium counts. The outlier value was changed to the mean count value for calcium 18 month mice.

Results

Descriptively, more plaques were measured from the male mice, two plaques per mice, and only one plaque per female mouse because the experimenters were blind to the sex of the mice during data collection. As seen in Table 2, there were many more cortical plaques than hippocampal plaques measured in the 12 month group.

Overall Comparisons

A 3x3x2 repeated measures analysis of variance (RMANOVA) was performed with metal, zinc, copper, or iron, as the repeated independent measure to determine if the concentration of metal in the amyloid plaques changed significantly as a function of age, (12 month, 18 month, and 22 month) or the plaques location within the brain (hippocampus and cortex). The dependent variable was the concentration of metal measured in parts per million. Refer to Table 2 to see all the means, standard deviations, and number of plaques used in the analyses and Figure 3 to see representative metal distributions.

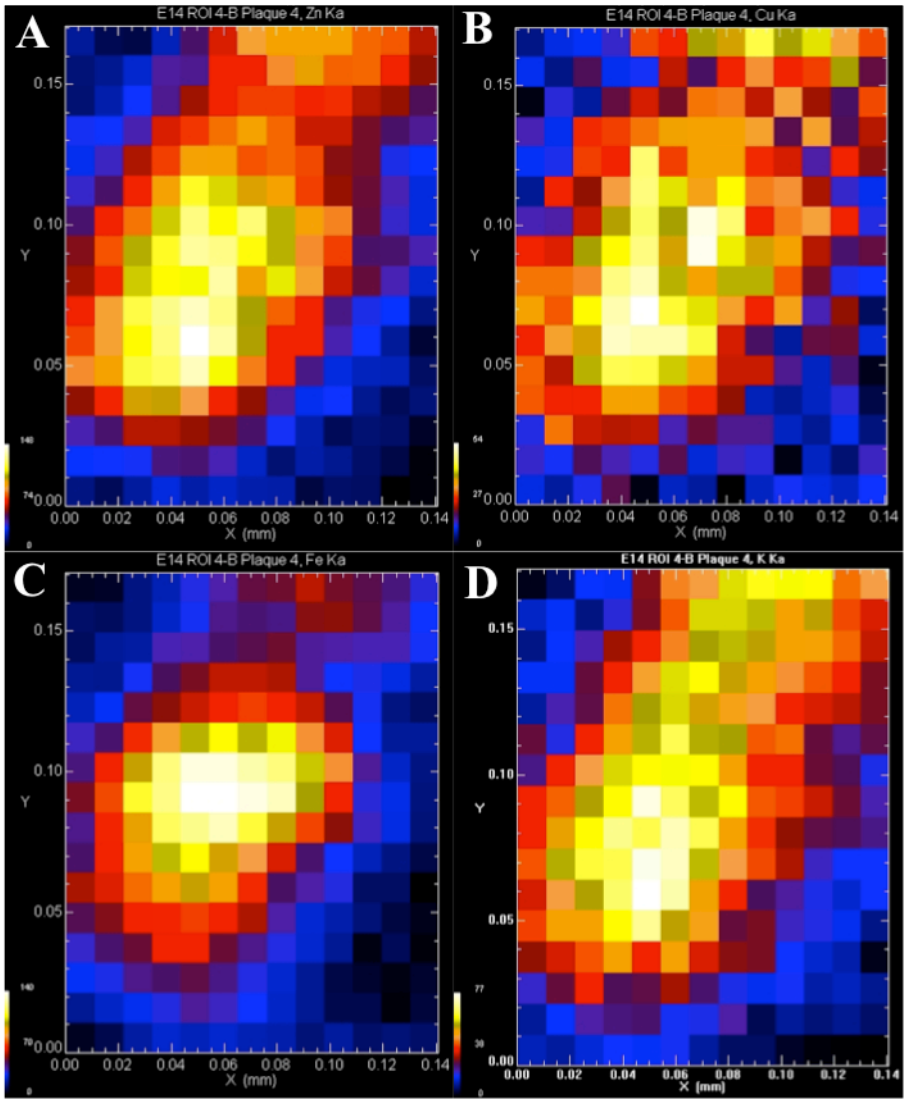

Figure 3. Representative metal output images for Zn, Cu, Fe, and K in one plaque. Output images of one plaque from a 18 month group mouse from the SXRF data plotting program. The color scale bar is determined by the program and is based on the counts for the individual element. **A)** Zinc **B)** Copper **C)** Iron **D)** Potassium

There was a significant difference found between the concentrations of metals ($F(2,58) = 28.38$, $p < .001$) in the overall multivariate test. A follow up Bonferonni post-hoc test found that there was significantly lower concentration of copper (M =7.43, SD =

6.89) than zinc (M = 65.70, SD = 55.32) and iron (M = 63.77, SD = 63.64), p > .00 (See Figure 4).

Table 2. Mean metal concentrations in the plaques of the different age groups, two brain regions, and overall.

12 months	**Overall**	**SD**	**N**	**Hippocampus**	**SD**	**N**	**Cortex**	**SD**	**N**
Zinc	59.81	59.66	15	43.39	94.29	4	65.78	66.21	11
Copper	9.98	8.23	15	4.00	3.00	4	13.01	8.12	11
Iron	135.86	48.88	15	28.82	4.97	4	108.97	50.10	11
Males			10						
Females			5						
18 months	**Overall**	**SD**	**N**	**Hippocampus**	**SD**	**N**	**Cortex**	**SD**	**N**
Zinc	72.33	21.83	16	68.60	21.71	8	76.06	22.76	8
Copper	9.02	5.93	16	8.88	6.31	8	9.15	5.97	8
Iron	66.40	46.40	16	75.48	49.69	8	57.31	44.22	8
22 months	**Overall**	**SD**	**N**	**Hippocampus**	**SD**	**N**	**Cortex**	**SD**	**N**
Zinc	64.18	60.40	34	52.84	13.07	16	75.98	87.68	18
Copper	5.45	6.06	34	6.55	6.07	16	5.40	6.31	18
Iron	50.84	62.14	34	52.10	42.76	16	51.94	82.21	18

There was no significant change in the total concentration of metals across the age-groups, ($F(4,118) = .60$, $p > .5$) as measured by the Pillai's Trace. There was no significant change in the total concentration of metals between the cortex and hippocampus ($F(2,58) = .573$, $p > .05$) as tested by Pillai's Trace method. The interaction between the change in the concentrations of the three metals, the age of the mice, and the location of the plaques in the brain was also not significant, ($F(4,118) = 1.52$, $p > .2$).

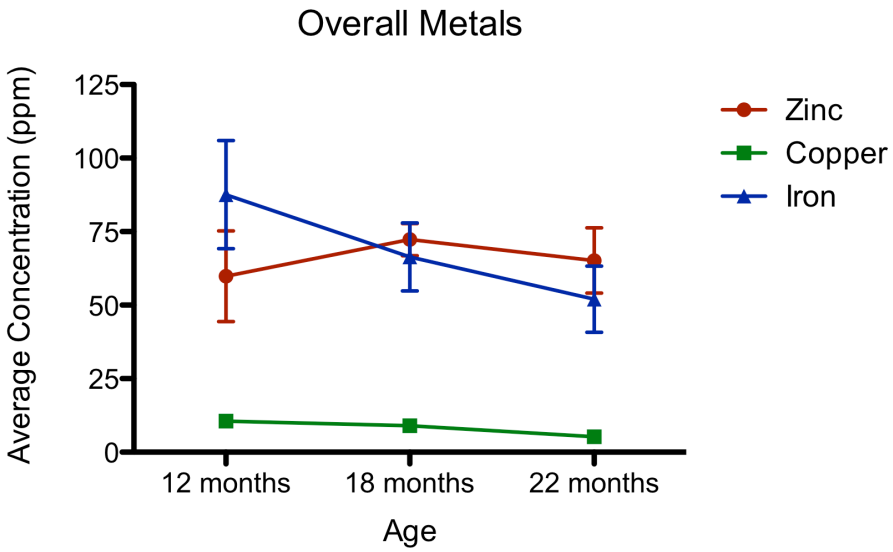

Figure 4. The average concentration in the plaques for each metal across the age groups. The mean concentration of each metal in the plaques for each age group. Error bars represent the standard error of the mean.

Individual Metal ANOVAs

Analysis of variance tests (ANOVA) were run individually for each metal, zinc, copper, or iron, with two independent variables, age, three levels: 12 months, 18 months, and 22 months, and brain area, two levels: hippocampus and cortex. There was no significant change in the concentration of zinc across the age groups ($F(2,64) = .333$, $p > .5$), between the two brain areas ($F(1,64) = 1.22$, $p > .2$), and the interaction between age and plaque location was also not significant ($F(2,64) = .107$, $p > .8$). It was hypothesized that the concentration of copper would stay the same or only decrease with age; however, there was no significant difference in the concentration of copper across the different age groups ($F(2,64) = 2.30$, $p > .1$). However, there was a trend toward a significant difference in the concentration of copper between the two brain areas, ($F(1,64) = 3.08$, $p = .085$), with the cortical plaques (M= 9.19) having a higher concentration of copper than the hippocampal plaques (M=6.01). A planned *a priori* post-hoc test was done to assess what age groups had significantly different concentrations of copper. A Bonferonni's test found that the concentration of copper in the 22 month age group (M = 5.23) was significantly lower than the concentration of copper in the 12 month age group (M = 10.88) ,$p = .03$ (See Figure 5).

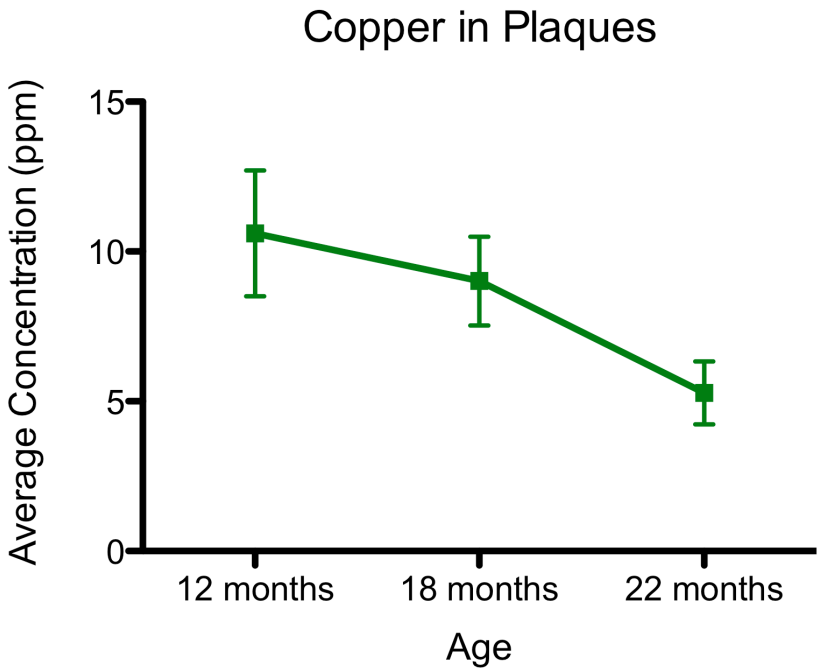

Figure 5. The average concentration of copper in hippocampal and cortical plaques. The mean concentration of copper in both hippocampal and cortical plaques is plotted across the three age groups. There was significantly less copper in the 22 month group plaques than the 12 month group plaques, $p < .03$. The error bars represent the standard error of the mean.

The interaction term between age and plaque location for copper was not significant, ($F(2,64) = 2.19$, $p > .1$). The hypothesis that the concentration of iron would increase significantly with age was not confirmed ($F(2,64) = .48$, $p > .6$). Additionally, there was no significant difference in the concentration of iron between the two brain areas ($F(1,64) = 1.41$, $p > .2$). Finally, the interaction between age and brain area was also not significant for iron ($F(2,64) = 2.42$, $p > .09$).

Cortex Differences

While performing the ANOVAs to ascertain whether there were significant differences in the concentration of the metals by age, brain area, or an interaction, a noticeable difference was seen in the cortical plaques across the age groups (See Figure 6).

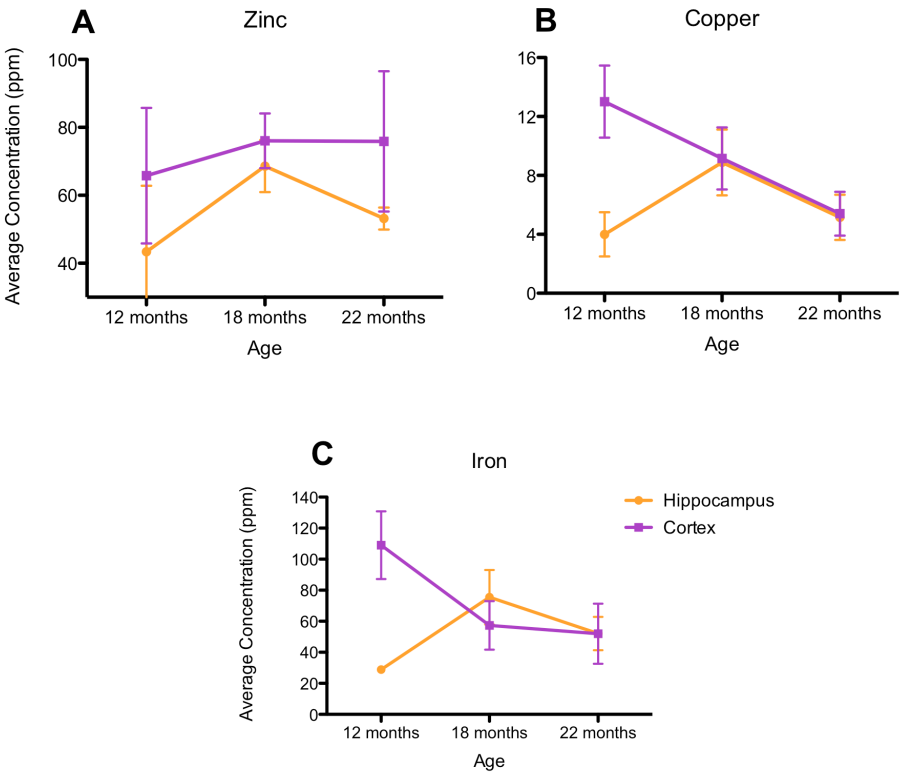

Figure 6. Average concentration of the three metals in the plaques across the three age groups split into brain area. The average concentration of each metal in the plaques is split into brain area and plotted across the three age groups. **A**: Zinc, **B**: Copper, **C**: Iron. The error bars represent the standard error of the mean.

Individual ANOVAs were run only on the cortical values for each metal with age as the independent variable (3 levels: 12 months, 18 mo00nths, and 22 months). There was no significant change in the concentration of zinc in cortical plaques across the age groups ($F(2,36) = .076$, $p > .9$). There was a significant change in the concentration of copper across the three age groups in the cortical plaques ($F(2,36) = 4.29$, $p < .03$). A follow up Tukey's HSD post hoc test revealed a significant decrease in the concentration of copper in the cortical plaques from the 12 month group (M = 13.01, SD = 8.12) to the 22 month group (M = 5.40, SD = 6.31), $p < .02$. There was no significant change in the concentration of iron across the age groups ($F(2,36) = 2.24$, $p > .1$). Individual metal ANOVAs were also run on the metal concentrations in only the hippocampal plaques to check for significant differences with age but none were found, zinc ($F(2,27) = 2.46$, $p > .1$), copper ($F(2,27) = 1.35$, $p > .2$), and iron ($F(2,27) = 1.74$, $p > .1$).

MCA Data

An individual ANOVA was run for each element from each of the two age groups 18 and 22 months, with two independent variables, age and brain area (hippocampus and cortex) and the counts for each element as the dependent variable. As expected in the 18 month age group, there was a significant difference in the counts for zinc between the plaque and non-plaque tissue, ($F(1,34) = 14.69$, $p < .001$). However there was no significant difference in the zinc counts between the cortex and hippocampus, ($F(1,34) = .244$, $p > .6$) or the interaction between the type of tissue and the brain area ($F(1,34) =$

.005, $p > .9$). Similarly there was a significant difference in the copper counts between plaque and non-plaque tissue in the 18 month mice ($F(1,34) = 9.12$, $p < .005$). As with the zinc counts, there was no significant difference between the copper counts in the hippocampus and cortex ($F(1,34) = .025$, $p > .8$) nor was there an interaction between the type of brain tissue and the brain area ($F(1,34) = .088$, $p > .7$). Again there was a significant difference in the iron counts between plaque and non-plaque brain tissue ($F(1,34) = 7.30$, $p < .02$). No significant difference in the iron counts was found between the two brain areas ($F(1,34) = .079$, $p > .7$) nor was there an interaction between the type of brain tissue and the brain area ($F(1,34) = .128$, $p > .7$). Although there was no *a priori* hypothesis for potassium, the difference between plaque and non-plaque tissue was notable and then analyzed. A trend towards a statistically significant difference between plaque and non-plaque was found in the potassium counts ($F(1,34) = 3.55$, $p < .07$). There was no significant difference between potassium counts in the hippocampus and the cortex ($F(1,34) = .637$, $p > .4$) nor was there an interaction between the brain areas and the tissue type ($F(1,34) = .695$, $p > .4$). There were no significant differences in the calcium counts between the plaque and non-plaque tissue ($F(1,34) = 1.67$, $p > .2$), or the different brain areas ($F(1,34) = .742$, $p > .3$), or the interaction between the type of tissue and the area of the brain ($F(1,34) = .022$, $p > .8$) (See Figure 7). The calcium counts may not be entirely reliable because the potassium Kβ energy peak can completely overlap the calcium Kα energy peak.

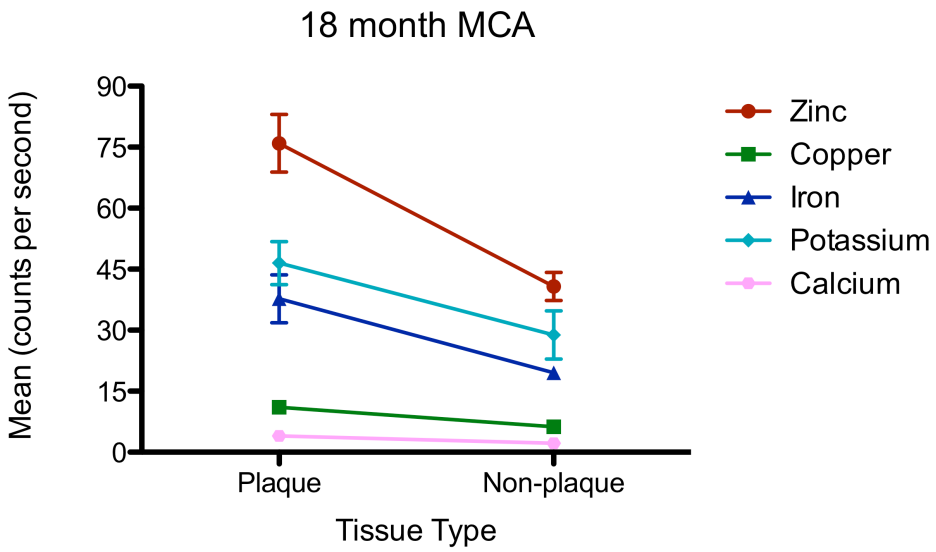

Figure 7. The average counts per second for each element in plaque and non-plaque brain tissue in the 18 month group. The mean counts per second for zinc, copper, iron, potassium, and calcium collected using the MCA technique. Error bars represent the standard error of the mean.

Since MCA data was collected on only non-plaque tissue in the 22 month age group, analyses can only be run to ascertain whether there are changes in the element counts between the different brain areas, the hippocampus and the cortex. It was hypothesized that no significant differences would be found in the counts between the two brain areas. As expected there was no significant difference in the counts of any of the elements in non-plaque tissue between the hippocampus and the cortex: zinc ($F(1,21) = .201$, $p > .6$), copper ($F(1,21) = .092$, $p > .7$), iron ($F(1,21) = .382$, $p > .5$), potassium ($F(1,21) = .601$, $p > .4$), or calcium ($F(1,21) = .233$, $p > .6$). See Figure 8.

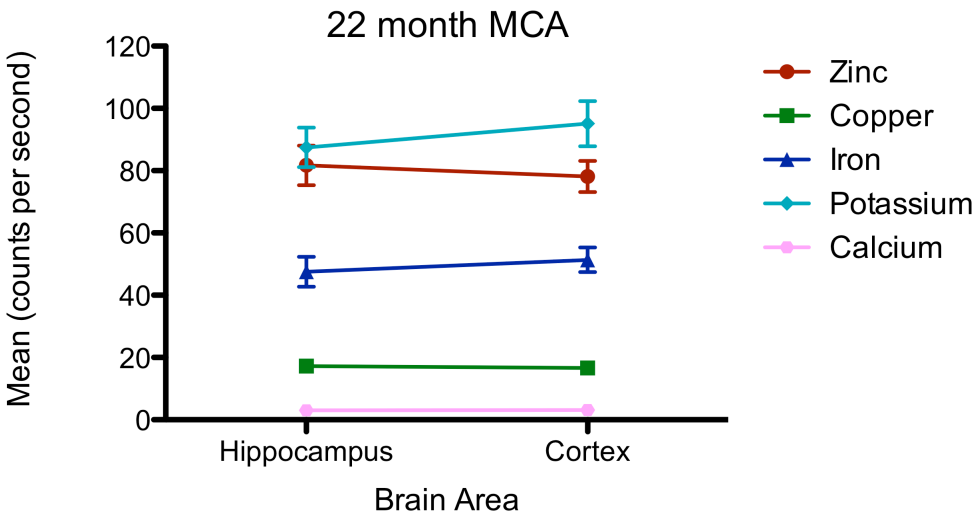

Figure 8. The average counts per second for each element in non-plaque brain tissue between two brain areas in the 22 month mice. The mean counts per second for zinc, copper, iron, potassium, and calcium from non-plaque tissue in the hippocampus and cortex of the 22 month mice.

Discussion

The overall aim of this study was to measure the concentration of metals in Aβ plaques in the Tg2576 mouse model of AD and investigate the effect of age on metal deposition in the amyloid beta plaques in a murine model of Alzheimer's disease. The metals, zinc, copper, and iron, are all necessary for normal brain development and function and found in relatively high levels in the brain. An advantage to this study is the use of SXRF technology, which allows for quantification of metals in plaques and can measure the whole elemental make up of a sample at once. There are only a few quantitative studies of metal concentration in mouse models of AD; they measured co-localization of the metals and plaques or whole brain concentration rather than concentrations in the plaques (Falangola et al., 2005; Lee et al., 1999). However, a study on human brain tissue affected with AD has found increased concentrations of zinc (1055 μM), copper (390 μM), and iron (940 μM) in the plaque tissue compared to the non-plaque tissue, zinc (350 μM), copper (70 μM), and iron (340 μM) (Lovell et al., 1998). In this study the counts of zinc, copper, and iron in the plaques of Tg2576 were also significantly higher than the concentration of the metals in non-plaque tissue. Lovell et al. (1998) also found significantly more zinc, copper, and iron in AD brains versus age-matched controls.. Additionally, the previous studies looking at metal content in human AD brains and AD mouse model brains have only looked at one time point, therefore it is

unknown whether zinc, copper, and iron in amyloid plaques increase or decrease with age and disease progression.

In human Alzheimer's disease, the tightly regulated homeostasis of zinc, copper, and iron in the brain seems to become imbalanced when compared to age-matched controls. One possible reason for the dysregulation is that the human amyloid precursor protein and Aβ peptide have multiple histidine-mediated binding sites for copper and zinc and translation of APP is up regulated with exposure to iron (Adlard & Bush, 2006). The binding of Aβ by zinc has been shown to change Aβ's conformation to α-helix and β-pleated sheet *in vitro* (Huang, Atwood, Moir, & Hartshom, et al., 1997), which causes the amyloid β to form plaques. Iron has also been shown to change Aβ's conformation into β-pleated sheet (House et al., 2004).

The primary hypotheses of metal concentration change over age were as follows: zinc in the amyloid plaques would not change significantly with age, iron in amyloid plaques would increase with age, while copper in the plaques would stay the same or decrease. It was thought that the concentration of iron would increase with age because as more amyloid β is released from APP and would form more plaques, which causes an increase in oxidative stress, more iron would be sequestered into the plaques. There was not a significant change in the average concentration of zinc in plaques across the three age groups. However, the change in the concentration of iron in the plaques across the ages was also not significant. Although the concentrations of zinc and iron do not change significantly with age, the number and size of the amyloid plaques do increase with age.

Thus, a decrease in the zinc and iron in the non-plaque brain tissue with age would be expected. It was thought that the average concentration of copper would decrease because as plaques age more Aβ1-40 is found in the plaques which is not as tightly bound to copper as Aβ1-42 (Maynard et al., 2002). The decrease in copper in the whole across all the age groups in the whole brain was not significant but an *a priori* post hoc test revealed a significant decrease in the concentration of copper in the plaques from 12 months to 22 months. Additionally the concentration of copper in cortical plaques showed a significant overall change, with a post-hoc test showing a significantly lower concentration of copper in the 22 month plaques compared to the 12 month plaques (See Figure 6).

Copper is an essential trace element, necessary for proper brain functioning, and is normally found as a part of different proteins, such as metallothioneins, Cu,Zn-superoxide dismutase, and dopamine β-hydroxylase (Hung, Bush, & Cherny, 2010; Suwalsky, Villena, Cardenas, Norris, Sotomayor & Zatta, 2003). Interestingly, the interaction of copper and Alzheimer's disease is complicated and multifaceted. Copper has been shown to associate with the β-secretase, BACE-1, which implicates a role for copper in the processing of APP (Hung et al., 2010). Borchadt, et al.(1999) suggests that the presence of increased copper promotes the non-amyloidogenic processing of APP and lessens Aβ production. Conversely, the increased presence of Aβ in the AD brain induces copper dishomeostasis in the brain, which can cause increased oxidative stress damage, Aβ aggregation, and plaque formation. In this study the concentration of copper in the plaques of Tg2576 decreased significantly with age and there was significantly

more copper in plaque tissue compared to non-plaque brain tissue in one age group. The effect of decreasing copper in the whole brain could lead to increased Aβ production in the surviving neurons through the amyloidogenic processing of APP and therefore increase the amount of plaques in the brain.

Another main focus of this study was to determine if the region of the brain where the plaques were located would have a significant effect on the concentration of each metal in the plaque. Also, the possibility of an interaction between age and location was investigated. There were no significant regional differences in the concentrations of zinc or iron in the plaques but the difference in the concentration of copper between plaques in the hippocampus and the cortex trended toward significance. Specifically, the amyloid β plaques in the cortex contained more copper than the hippocampal plaques (see Figure 6). There were also no significant interactions between age and brain area for any of the metals. This is probably because of an unequal number of hippocampal and cortical plaques measured, especially in the 12 month age group.

One of the many advantages of using the Synchrotron X-ray Fluorescence technology is that it is possible to measure all of the elements in a substrate at one time using different techniques. Multi-channel analyses were taken from plaque and non-plaque brain tissue in the 18 month old mice. The MCA counts for zinc, copper, and iron were significantly different between plaque and non-plaque brain tissue in the 18 month group, as would be expected based on previous studies (Lee et al., 1999; Maynard et al., 2002; Smith et al., 1998). The difference in the potassium counts between plaque (M =

46.51, SD = 23.07) and non-plaque (M = 28.83, SD = 23.70) brain tissue trended towards significance (see Figure 9). The finding of increased potassium in plaque tissue in a mouse model of AD is novel and relates to work being done in neuron culture models. Two groups have hypothesized that increasing concentrations of amyloid β can cause different ion channels to open, including potassium channels. This continual flooding of potassium ions can cause neuronal death in an *in vitro* neuron culture model (Salminen, Ojala, Suuronen, Kaarniranta & Kauppinen, 2008; Wilcock, Vitek, & Colton, 2009). The counts for calcium were not significantly different between plaque and non-plaque tissue in the 18 month old mice. Although MCAs were collected for the 22 month mice, they were only taken from non-plaque tissue so it is not possible to look at any differences between plaque and non-plaque tissue in the older mice. Additionally, the sheep brain standards spiked with the different elements were not run with the MCA technique either, so comparisons between the counts in the non-plaque tissue from the 18 month and 22 month mice were not possible.

As seen in humans, Tg2576 mice, and other murine models of Alzheimer's disease, there were increasing numbers of plaques in the older age groups (Braak & Braak, 1991; personal observation). In the 12 month age group, data from 15 plaques were taken from 9 mice. Although data was collected from only one more plaque (16) in the 18 month age group, the plaques came from 5 mice. Finally, data from 34 plaques in 9 mice was collected in the 22 month age group. It was not possible to collect data from all of the plaques or even a large percentage of the plaques in each animal because of time constraints during data collection. Please refer to Figures A6-A8 in the Appendix

for representative brain slice images from each age group to assist in visualizing the increase in the number of plaques with age. The increasing number of plaques with age and the statistically significant increase in counts of zinc, copper, and iron in the amyloid plaques in the Tg2576 mice of this study are similar to findings in studies of human AD brain tissue and add validity to the Tg2576 model of Alzheimer's disease. Additionally, the increase in the number of plaques with age means more metals are sequestered from the non-plaque tissue and thus the metals may decrease with age.

This study is different from previous studies looking at metals in AD brains because of the use of SXRF, the method used to collect the elemental data in the plaque and non-plaque brain tissue. Synchrotron X-Ray fluorescence was chosen because it has many advantages over the traditional methods used to investigate trace elements in tissue. Most importantly, SXRF technology gives quantitative counts for each element in the sample, unlike the qualitative differences seen with histopathological staining. This allowed for direct observations of the elements in individual plaques, which is different than previous studies looking at overall brain metal content. Additonally, it does not damage the substrate, like Particle Induced X-ray Emission (PIXE), therefore multiple different plaques or areas of tissue can be run at different times. It is also possible to run the same piece of tissue more than once. Also, it is possible to look at many elements at the same point or over the same areas at the same time. This allows one to search for elemental changes that might not have been expected, like the change in potassium counts between plaque and non-plaque brain tissue seen in the 18 month mice MCAs in this study. Finally, although it is possible to use different stains to identify the elements

with in the sample, such as Prussian Blue for iron, fixing and staining the fresh tissue can wash away unbound elements in the tissue and therefore affect the amount of elements that are able to be measured.

As with any study or set of experiments, this study had limitations that need to be addressed. First, data from only a limited number of plaques and non-plaque tissue areas was able to be collected. Each plaque can take anywhere from 20 minutes to 3 hours to run, which does not include the time to set up the beam for data collection, find the plaques in the section, and intermittent beam dumps (times when the beam does not have proper stability and signal and is purged and refilled with energy). All of these factors decrease the little concentration of time that is granted for each data collection run at the National Synchrotron Light Source. The addition of more data on the plaques from each age group, tissue type, and brain area could help illustrate the true story of what is happening to zinc, copper, and iron in the brains of an AD mice model. Secondly, because data collection is time limited, samples from the different age groups were run during different collection sessions. The x-ray beam set up and the resulting data peaks were slightly different for each run, which may be the cause of the high variation in some of the metal concentrations. However, the sheep brain standards, which were made fresh for every run, this should have allowed for accurate calibration of the metal concentrations.

There were some key data points missing that would have made this story more complete. No MCA data was collected for the 12 month age group for either plaque or

non-plaque tissue or the 22 month plaque tissue. The addition of this data, along with MCA standard curves, would have allowed for analyses on change of the elemental content across the ages, between tissue types, and the interaction of age and tissue. Noticeably, there was no metal concentration data collected from the wild type littermate control mice. This data would have been nice to compare with the MCAs from the non-plaque tissue in the transgenic animals to ascertain whether the concentration of zinc, copper, iron, potassium, or calcium is different between wild type mice and Tg2576 mice. Additionally, it would have been possible to determine what effect age has on the concentration of metals and other elements in the wild type brains and compare that to the transgenic mice. Also, the possibility of finding regional differences between wild type and transgenic AD mice would have been present.

Conclusion

The ability to quantify the concentration of metals in the plaques of the Tg2576 mice with SXRF technology is a major advantage of this study. The key finding of a change in the concentrations of zinc, copper, and iron in the plaques of an AD mouse model as a function of age is novel. Interestingly, the different metals behave in different ways as the mice age. The finding of significantly higher counts of zinc, copper, iron, and potassium in the plaque tissue versus the non-plaque tissue of Tg2576 mice is similar to previous reports in human AD brains. Finally, the novel finding of increased potassium counts in the plaque tissue compared to the non-plaque brain tissue could be a key to high levels of neuronal death found in AD.

Appendix 1

Figure A1

Region of Interest 1: Interaural .64, Bregma -3.16

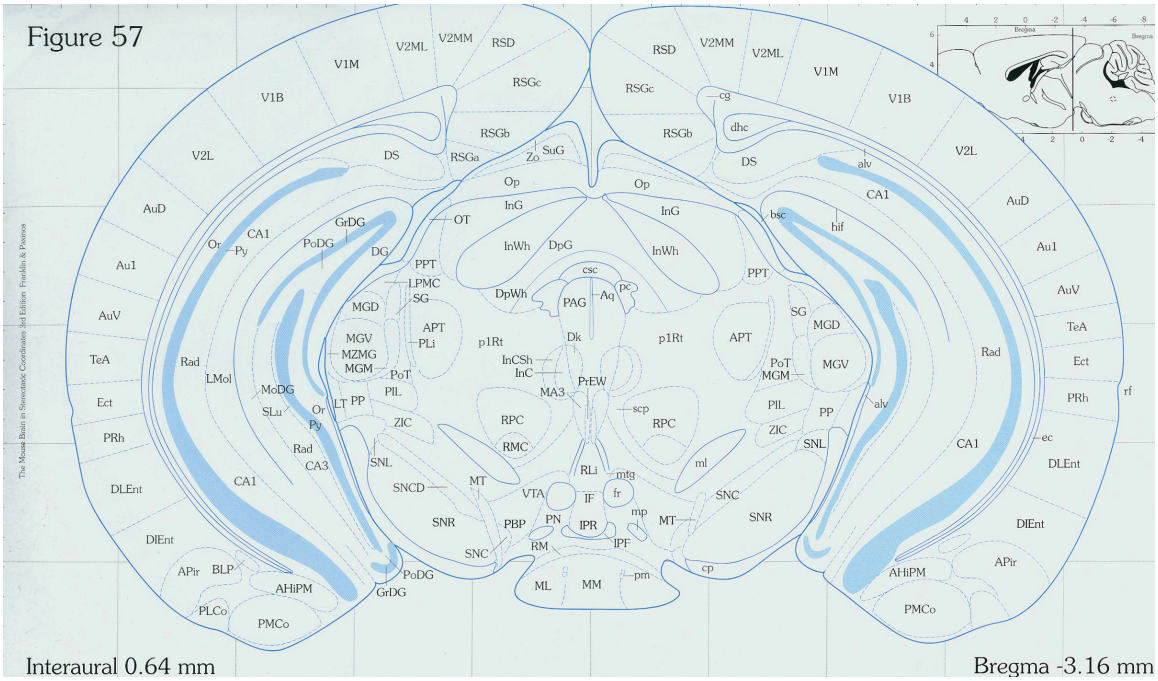

Figure A2

Region of Interest 2: Interaural 1.74, Bregma -2.0

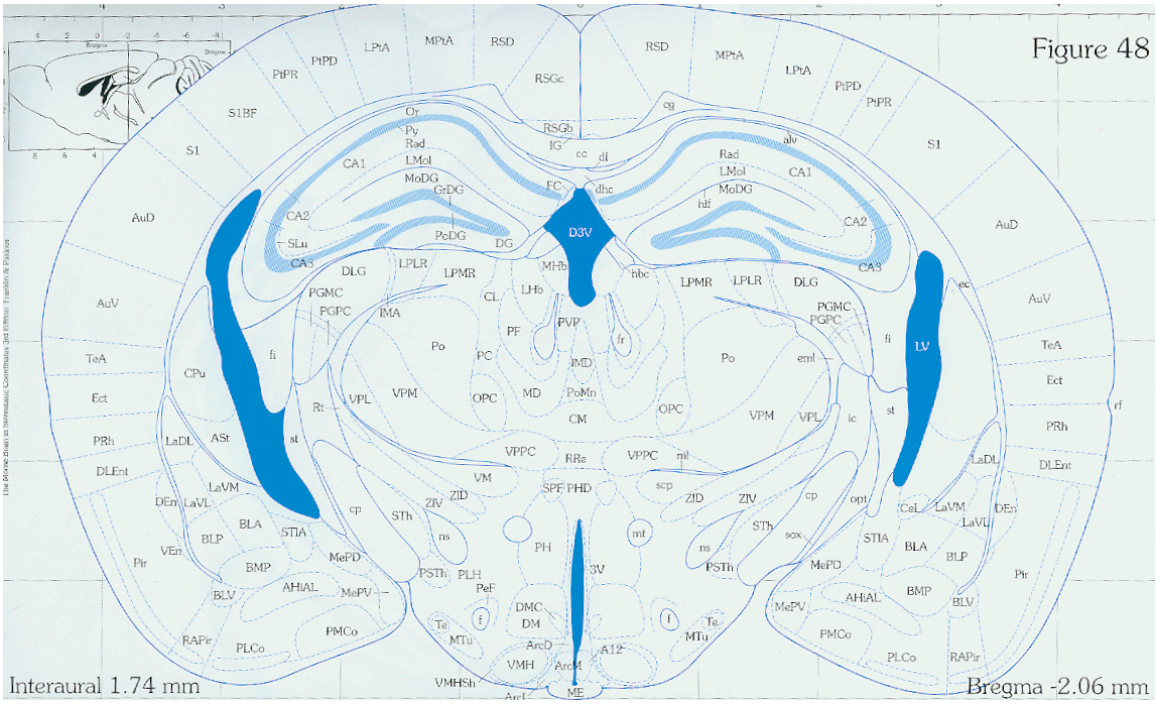

Figure A3

Region of Interest 3: Interaural 2.34, Bregma -1.46

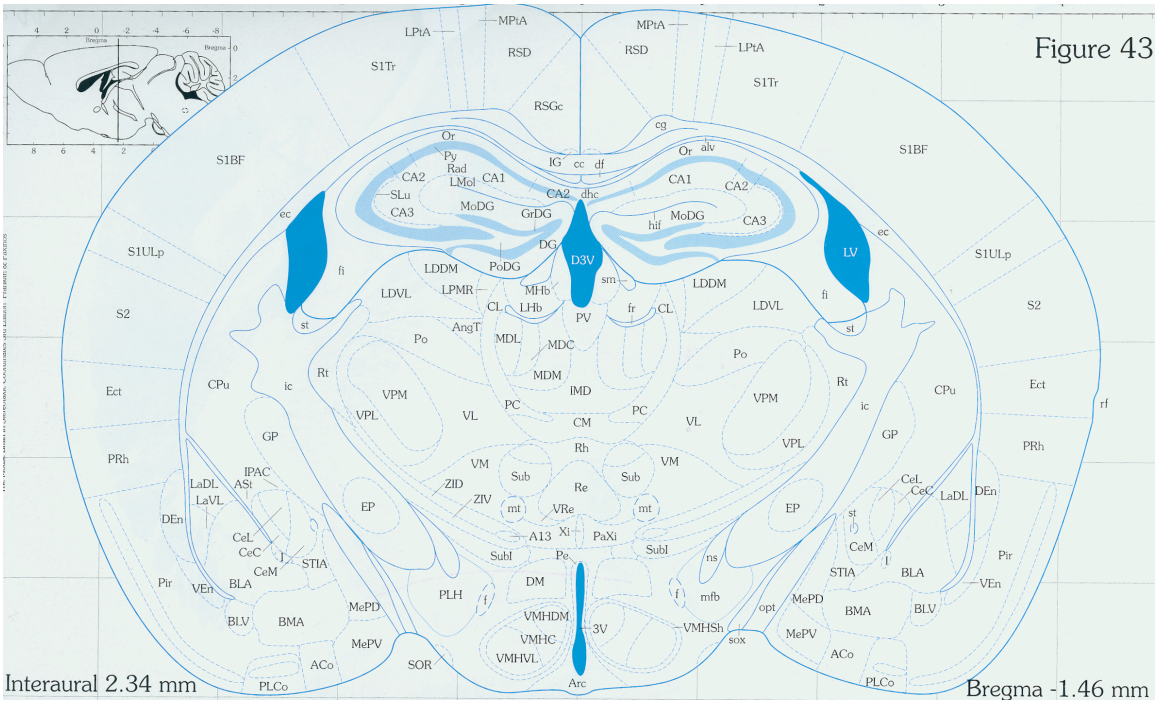

Figure A4

Region of Interest 4: Interaural 3.1, Bregma -.70

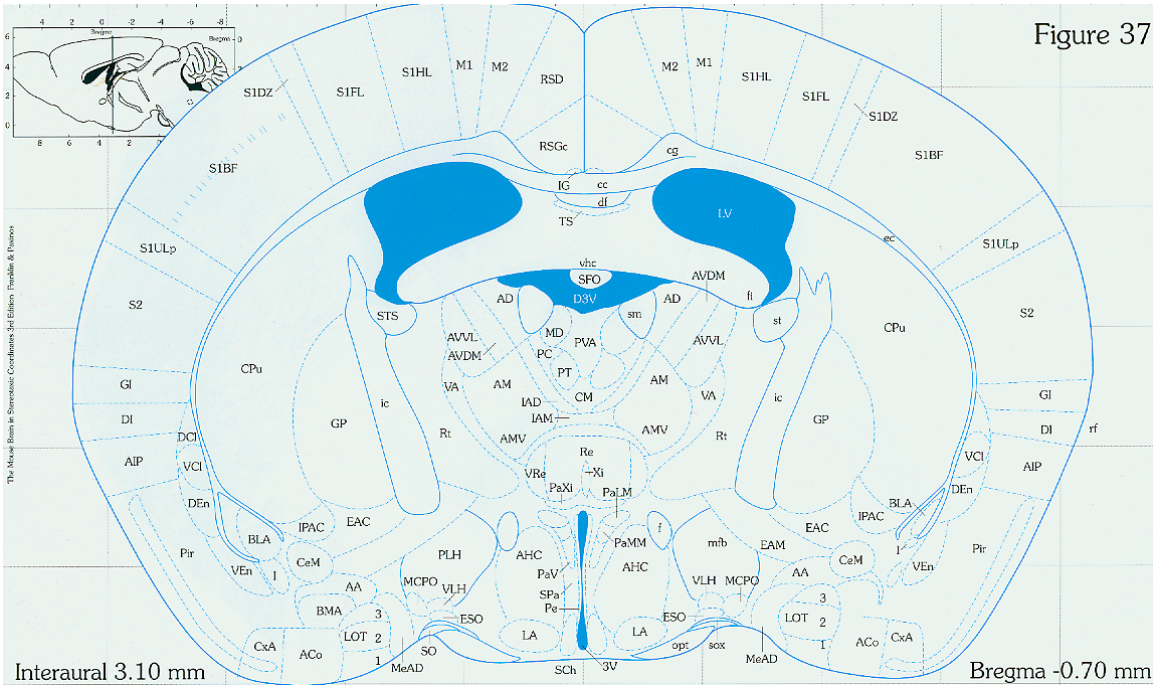

Figure A5

Region of Interest 5: Interaural 4.54, Bregma .74

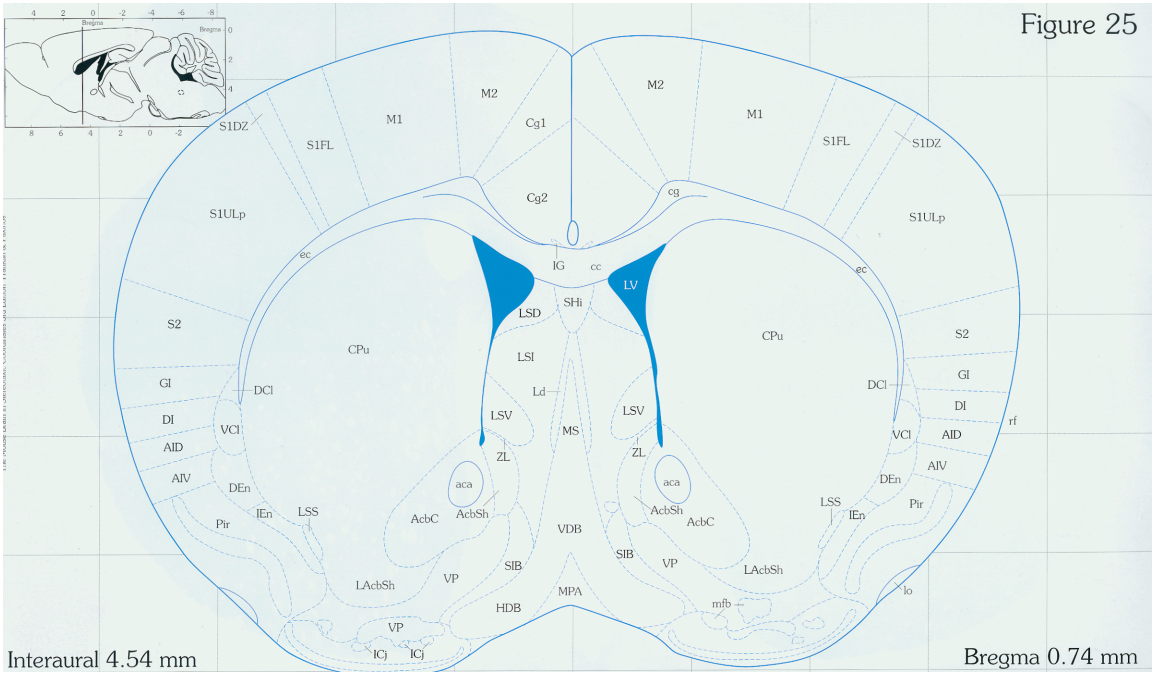

Figure A6

Representative brain slice from a 12 month old Tg2576 mouse.

Figure A7

Representative brain slice from a 18 month old Tg2576 mouse

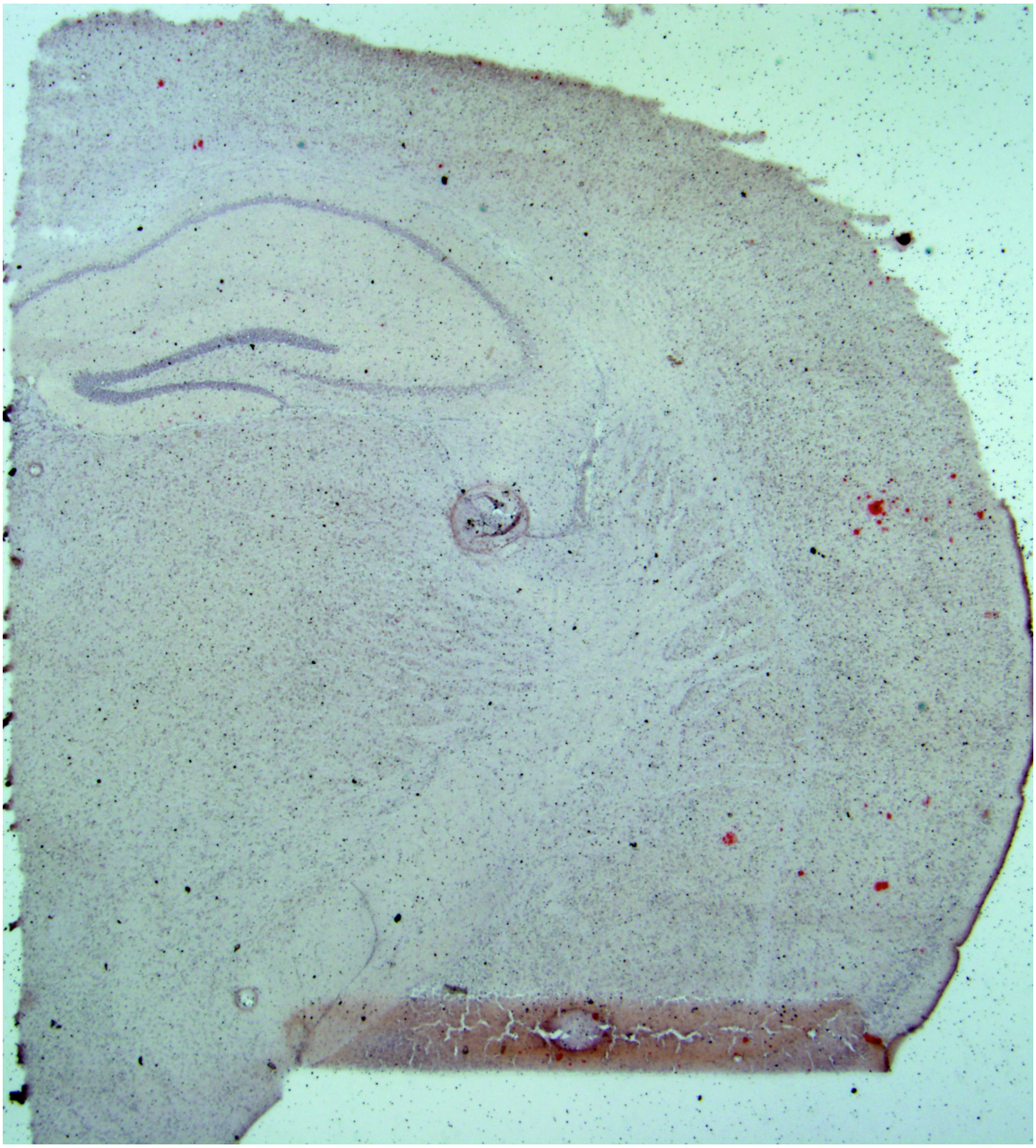

Figure A8

Representative image from a 22 month old Tg2576 mouse

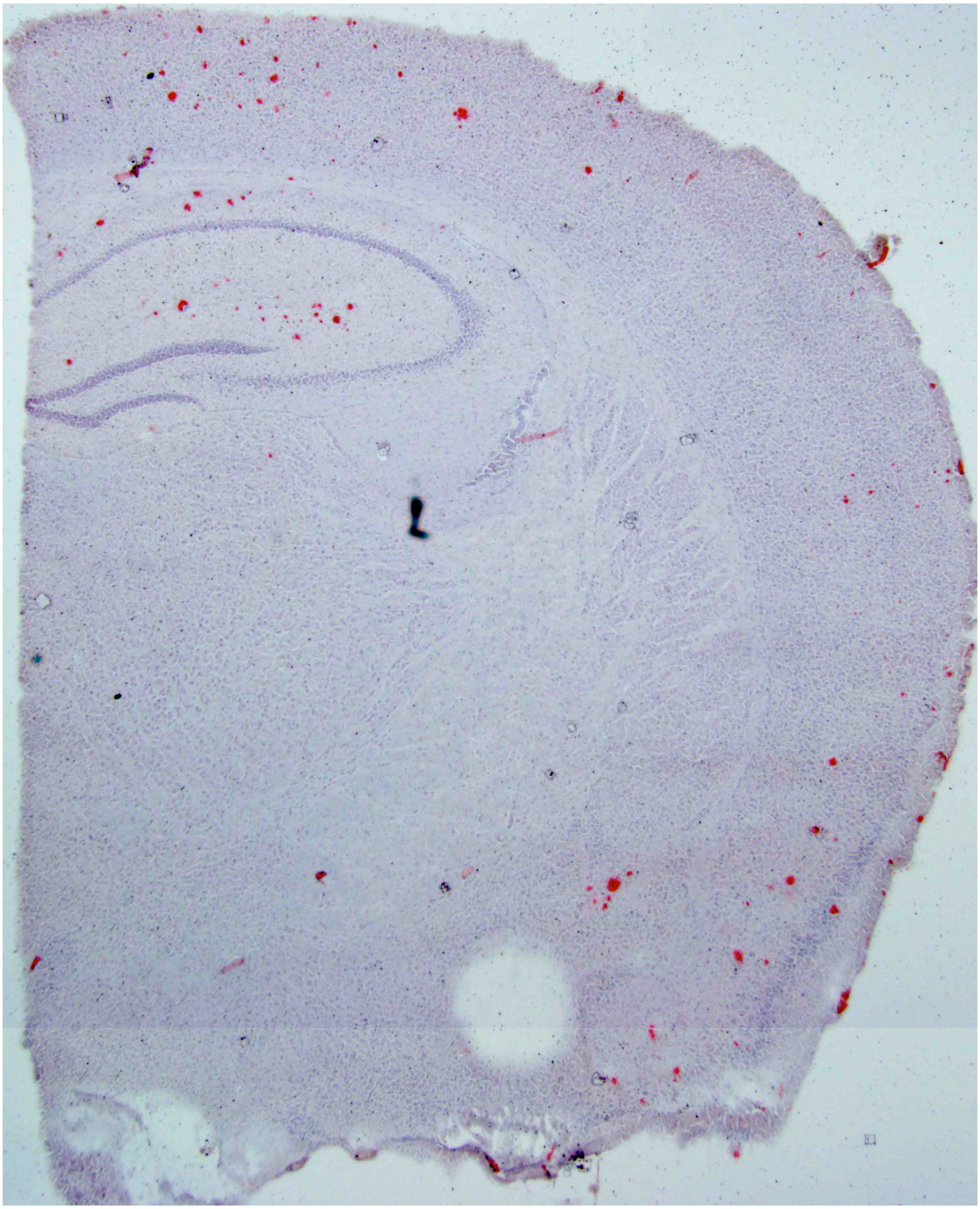

Appendix 2

Table A1

The means and standard deviations of the concentrations of zinc, copper, and iron in the plaques in 12 month old mice split by sex.

12 month old mice

	Zinc			Copper			Iron		
	Mean	SD	N	Mean	SD	N	Mean	SD	N
Male	76.73	66.45	10	13.25	8.49	10	97.01	81.76	10
Female	25.98	19.52	5	5.32	4.04	5	68.77	45.99	5

Table A2

Average metal concentrations in the cortical plaques across the ages.

	Cortical plaques								
	12 months			18 months			22 months		
	Mean	SD	N	Mean	SD	N	Mean	SD	N
Zinc	65.78	66.21	11	76.06	22.76	8	75.88	87.71	18
Copper	13.01	8.12	11	9.15	5.97	8	5.40	6.31	18
Iron	108.97	72.36	11	57.31	44.22	8	51.94	82.21	18

Table A3

Original Data Set

Brain area: 1-hippocampus, 2-cortex, 3-basal ganglia

Cohort 3	**12 months**									
Filename	Animal	Sex	ROI	Brain Area	Zinc cps	Zn ppm	Cu cps	Cu ppm	Fe cps	Fe ppm
Fall 2006										
c3_1_suspectCAA.001	c3	male	ROI 1	2	229.39	101.61	94.66	25.93	76.82	97.07
c3_2_corticalplaque.001	c3	male	ROI 2	2	159.01	59.21	79.08	17.66	74.17	92.01
c22_3_corticalplaque1.001	c22	male	ROI 3	2	1774.19	1032.15	81.29	18.83	116.38	172.47
c22_3_corticalplaque2.001	c22	male	ROI 3	2	2013.92	1176.56	79.93	18.11	115.32	170.45
c41_5_possibleplaque.001	c41	male	ROI 5	2	155.26	56.95	78.98	17.60	57.77	60.74
c41_5_possibleplaque2.001	c41	male	ROI 5	2	471.43	247.40	80.37	18.34	77.52	98.39
d2_3_corticalplaque1.002	d2	female	ROI3	2	103.39	25.71	54.82	4.78	52.09	49.92
d2_3_corticalplaque2.001	d2	female	ROI3	2	105.78	27.14	54.62	4.67	50.48	46.85
d2_5_bgplaque.001	d2	female	ROI 5	3	89.96	17.61	47.06	0.66	84.04	110.82
d19_2_corticalplaque.001	d43	female	ROI 2	2	156.23	57.54	67.13	11.32	65.20	74.92
d30_5_corticalplaque.001	d30	female	ROI 5	2	76.82	9.70	56.82	5.84	54.79	55.08
Spring 2008										
d1.002	d1	female	ROI 4	2	75.5375	9.82	undefined	0	59.85	10.77
c34.002	c34	male	ROI 3	1	296.928	101.00	undefined	0	120.63	26.26
Summer 2006										
c42_plaque.001	c42	male	ROI1	1	119.559	32.54	58.888	7.28	42.3048	34.28
c42_plaque.003	c42	male	ROI3	1	101.364	18.17	54.3298	4.50	37.9648	23.27
c42_plaque.004	c42	male	ROI2	1	106.019	21.84	53.8431	4.21	41.2029	31.48
Cohort 4	**18 months**									
e13.001	e13	female	ROI 2A #3	1	83.89	29.87	44.47	6.39	33.51	26.55
e13.003	e13	female	ROI 3B #4	2	127.61	79.66	undefined	0.00	34.28	28.04
e14.001	e14	female	ROI 4B #4	2	111.22	60.99	45.41	6.85	100.24	155.87
e28.001	e28	female	ROI 2A #11	1	117.89	68.59	undefined	0.00	80.12	116.88
e28.002	e28	female	ROI 2A #7	1	135.09	88.18	undefined	0.00	48.74	56.07
e28.003	e28	female	ROI 2B #11	2	131.63	84.24	49.92	9.05	51.51	61.44
e28.004	e28	female	ROI 3A #12	2	132.42	85.14	48.08	8.15	33.97	27.44
e28.005	e28	female	ROI 3A #9	1	137.60	91.03	50.39	9.28	59.54	77.00
e28.006	e28	female	ROI 3B #1-A	1	116.94	67.50	66.70	17.25	110.47	175.69
e28.008	e28	female	ROI 4A #2	2	87.40	33.86	44.46	6.38	30.55	20.82
e91.001	e91	female	ROI 2A #1	2	157.73	113.97	74.16	20.90	60.48	78.81
e91.003	e91	female	ROI 2B #2	2	121.25	72.42	49.87	9.03	42.59	44.15
e91.004	e91	female	ROI 3A	1	97.64	45.53	56.68	12.36	35.00	29.43

			#6							
			ROI 2A							
e92.001	e92	female	#9	1	119.19	70.07	57.96	12.98	56.78	71.64
			ROI 2B							
e92.002	e92	female	#2	2	126.30	78.16	57.70	12.85	41.42	41.88
			ROI 3B							
e92.003	e92	female	#6	1	134.92	87.98	57.58	12.80	45.93	50.62
Cohort 5	**22 months**									
			ROI 3B							
e27.008	e27	female	#1	1	169.685	51.82	55.38	12.38	98.79	41.80
			ROI 1							
e31.001	e31	female	#1	1	151.022	45.99	48.41	9.77	125.55	58.49
			ROI 2A							
e31.002	e31	female	#1	1	194.547	59.59	undefined	0.00	297.85	165.92
			ROI 2B							
e31.003	e31	female	#1	1	266.79	82.15	56.31	12.73	96.64	40.46
			ROI 3A							
e31.004	e31	female	#1	1	90.5911	27.12		0.00		0.00
			ROI 1							
e33.001	e33	female	#1	2	148.727	45.28		0.00		0.00
			ROI 2A							
e33.002	e33	female	#1	2	1366.17	425.49		0.00	633.33	375.10
			ROI 2B							
e33.003	e33	female	#1	2	183.128	56.02	60.71	14.38	93.59	38.56
			ROI 3A							
e33.004	e33	female	#1	2	188.443	57.68	60.03	14.12	116.58	52.89
			ROI 4A							
e33.006	e33	female	#1	3	182.758	55.91	50.83	10.68	172.74	87.91
			ROI 4B							
e33.007	e33	female	#1	2	191.253	58.56	48.86	9.94	70.20	23.97
			ROI 1							
e48.001	e48	female	#1	1	122.967	37.23		0.00	179.14	91.90
			ROI 2A							
e48.002	e48	female	#1	2	162.13	49.46		0.00	84.90	33.14
			ROI 2B							
e48.003	e48	female	#1	1	162.898	49.70	55.58	12.45	83.02	31.97
			ROI 3A							
e48.004	e48	female	#1	2	189.072	57.88	56.50	12.80	95.43	39.71
			ROI 4A							
e48.006	e48	female	#1	1	215.593	66.16		0.00	95.53	39.77
			ROI 4B							
e48.007	e48	female	#1	2	180.597	55.23		0.00	129.68	61.07
e49.001	e49	female	ROI 1 1	1	150.542	45.84		0.00	86.63	34.22
			ROI 3A							
e49.033	e49	female	#1	1	129.205	39.18	47.15	9.30	83.97	32.56
			ROI 5A							
e49.007	e49	female	1	2	162.801	49.67		0.00	77.63	28.61
			ROI 1							
e52.001	e52	female	#1	2	242.279	74.49	53.63	11.73	80.19	30.20
e52.002	e52	female	ROI 2A	1	179.081	54.76	60.18	14.18	88.23	35.22

e52.002	e52	female	ROI 2A #1	1	179.081	54.76	60.18	14.18	88.23	35.22
e52.003	e52	female	ROI 2B #1	2	157.381	47.98		0.00	110.11	48.86
e52.004	e52	female	ROI 3A #1	2	148.003	45.05		0.00	79.07	29.51
e52.005	e52	female	ROI 3B #1	1	188.327	57.65	53.36	11.63	75.14	27.06
e52.006	e52	female	ROI 4A #1	2	175.012	53.49	48.09	9.65	69.00	23.23
e52.007	e52	female	ROI 4B #1	1	149.126	45.40		0.00	116.71	52.98
e55.001	e55	female	ROI 1 #1	2	170.587	52.10		0.00	245.36	133.19
e55.002	e55	female	ROI 2A #1	2	232.074	71.31	55.14	12.29	82.67	31.75
e55.003	e55	female	ROI 2B #1	3	167.486	51.14		0.00		0.00
e55.005	e55	female	ROI 4B #1	3	252.934	77.82		0.00	111.65	49.82
e55.006	e55	female	ROI 5 #1	1	198.03	60.68		0.00	103.73	44.88
e56.005	e56	female	ROI 3B #1	3	193.187	59.16		0.00	79.01	29.47
e56.006	e56	female	ROI 4A #1	3	150.165	45.73		0.00		0.00
e56.007	e56	female	ROI 4B #1	2	152.001	46.30		0.00	82.31	31.53
e57.001	e57	female	ROI 1 #1	1	203.995	62.54	53.51	11.68	100.78	43.04
e57.002	e57	female	ROI 2B #1	2	232.557	71.46	55.20	12.31	82.74	31.79
e57.003	e57	female	ROI 3B #1	1	194.426	59.55	50.60	10.59	77.57	28.57
			ROI 4B							

Appendix 3

Figure A9

Standard curve graphs for sheep brain standards for the 12 month group mice

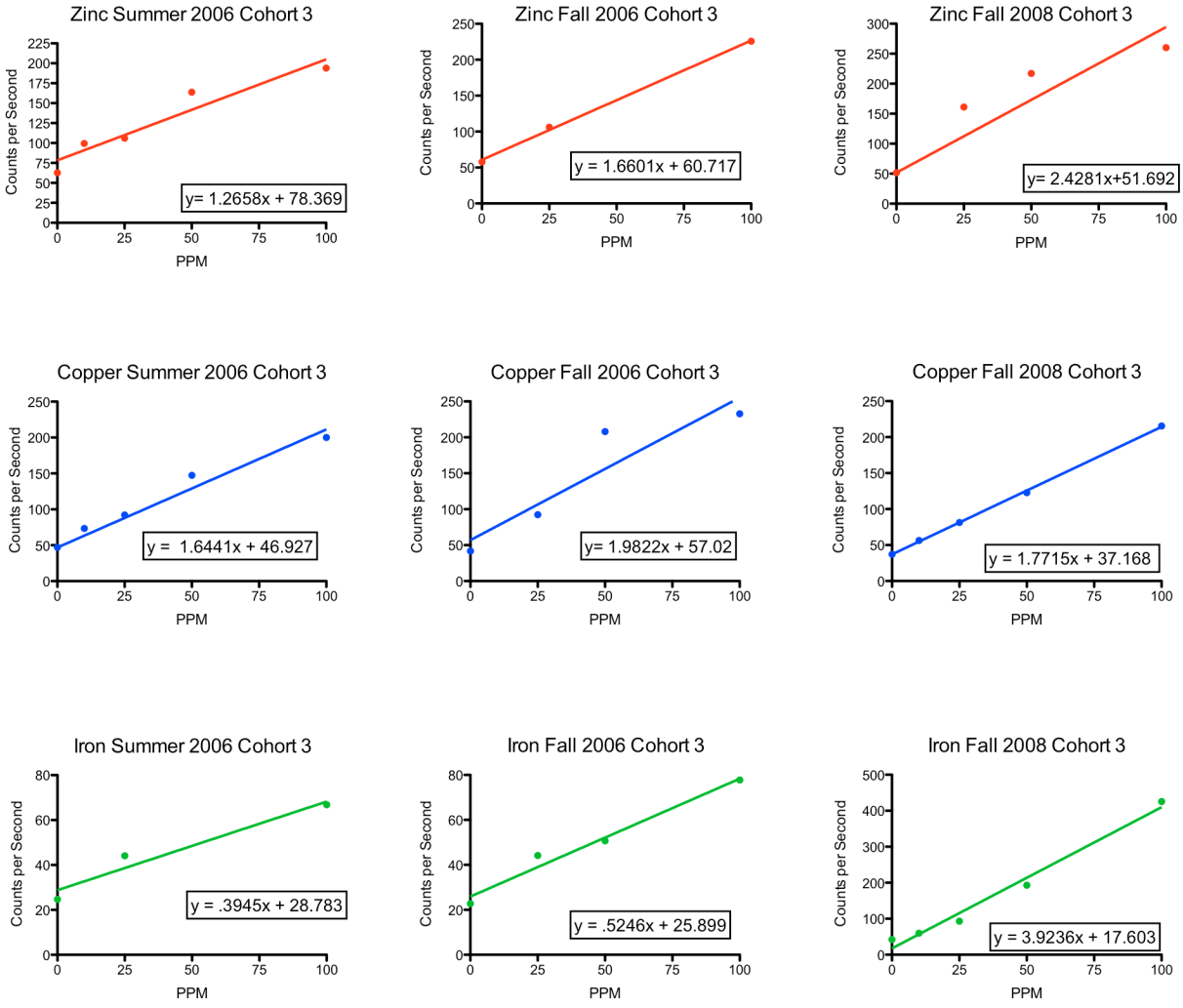

Figure A10

Standard curve graphs for sheep brain standards for the 18 month group mice

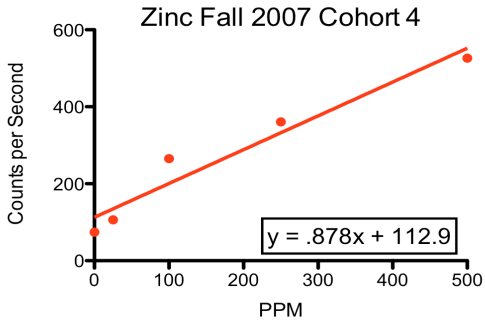

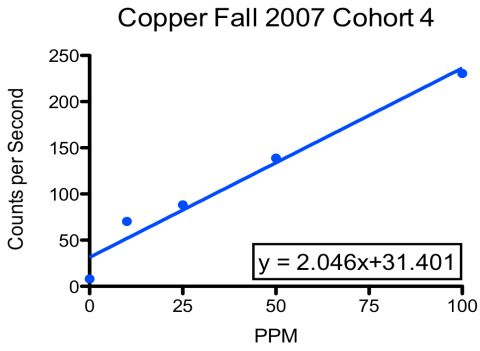

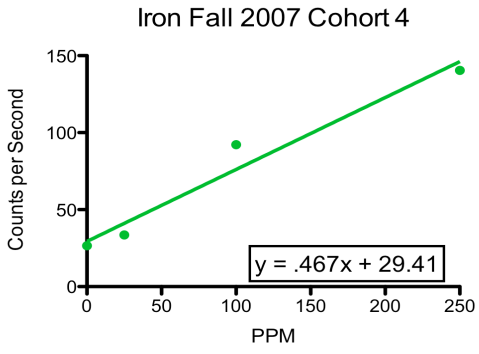

Figure A11

Standard curve graphs for sheep brain standards for the 22 month group mice

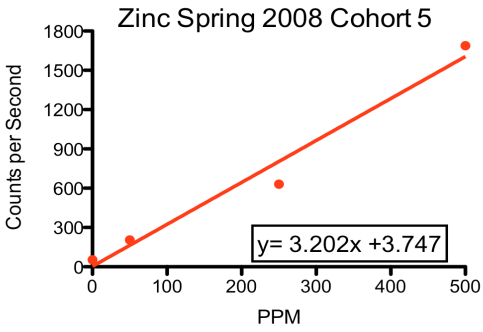

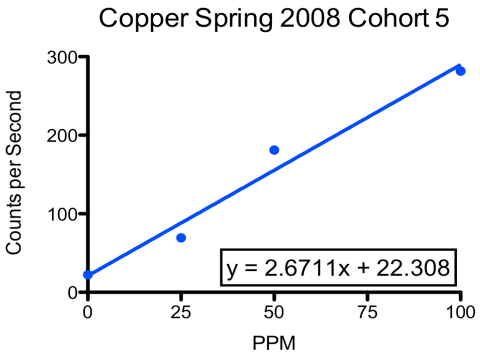

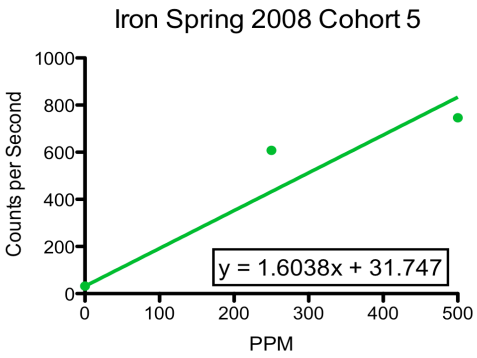

References

References

Adlard, P.A. & Bush, A.I. (2006). Metals and Alzheimer's disease. *Journal of Alzheimer's Disease, 10,* 145-163.

Ashe, K.H. (2001) Learning and memory in transgenic mice modeling Alzheimer's disease. *Learning and Memory, 8,* 301-308.

Atwood, C.S., Moir, R.D., Huang, X., Scarpa, R.C., Bacarra, N.M., & Romano, D.M. et al. (1998). Dramatic aggregation of Alzheimer abeta by Cu(II) is induced by conditions representing physiological acidosis. *Journal of Biological Chemistry, 273(21),* 12817-12826.

Bayer, T.A., Wirths O., Majtenyi K., Hartmann T., Multhaup G., & Bayreuther K. et al. (2001). Key factors in Alzheimer's disease: beta-amyloid precursor protein processing, metabolism, and intraneuronal transport. *Brain Pathology, 11(1),* 1-11.

Beher, D., Hesse, L., Masters, C.L., & Multhaup, G. (1996). Regulation of amyloid precursor protein (APP) binding to collagen and mapping of the binding sites on APP and collagen type I. *Journal of Biological Chemistry, 271,* 1613-1620.

Bennet, D.A., Wilson, R.S., Schneider, J.A., Evans, D.A., Aggarwal, N.T., Arnold, S.E., & Cochran, E.J. et al. (2003). Apolipoprotein E {epsilon} 4 allele, AD pathology, and the clinical expression of Alzheimer's disease. *Neurology, 60(2),* 246-252.

Borchardt, T., Camakaris, J., Cappai, R., Masters, C.L., Beyreuther, K., & Multhaup, G. (1999) Copper inhibits β-amyloid production and stimulates the non-amyloidogenic pathway of amyloid-precursor-protein secretion. *Biochemical Journal, 344,* 461-467.

Braak, H. & Braak, E. (1991). Neuropathological stageing of Alzheimer-related changes. *Acta Neuropathologica, 82,* 239-259.

Brown, A.M., Tummolo, D.M., Rhodes, K.J., Hofmann, J.R., Jacobsen, J.S., & Sonnenberg-Reines, J. (1997) Selective aggregation of endogenous beta-amyloid peptide and soluble amyloid precursor protein in cerebrospinal fluid by zinc. *Journal of Neurochemistry, 69,* 1204-1212.

Bush, A.I. (2003) The metallobiology of Alzheimer's disease. *TRENDS in Neurosciences, 26(4)*, 207-214.

Bush, A.I. (2008). Drug development based on the metals hypothesis of Alzheimer's disease. *Journal of Alzheimer's Disease, 15,* 223-240.4

Cedazo-Minguez, A. & Cowburn R.F. (2001) Apolipoprotein E: a major piece in the Alzheimer's disease puzzle. *Journal of Cellular and Molecular Medicine, 5(3),* 254-266.

Chai, C.K. (2007). The genetics of Alzheimer's disease. *American Journal of Alzheimer's Disease and Other Dementias, 22(1),* 37-41.

Chapman, P.F., Falinska, A.M., Knevett, S.G., & Ramsay, M.F. (2001). Genes, models, and Alzheimer's disease. *Trends in Genetics, 17(5),* 254-261.

Chayer, C. & Freedman, M. (2007). Frontal lobe functions. *Current Neurology and Neuroscience Reports, 1(6),* 547-552.

Corder, E.H., Saunders, A.M., Strittmatter, W.J., Schmechel, D.E., Gaskell, P.C., Small, G.W., & Roses, A.D. et al. (1993). Gene dose of apolipoprotein E type 4 allele and the risk of Alzheimer's disease in late onset families. *Science, 261(5123),* 921-923.

de Strooper, B., Saftig, P., Craessaerts, K., Vanderstichele, H., Guhde, G., Annaert, W., & Von Figura, K., et al. (1998). Deficiency of presenilin-1 inhibits the normal cleavage of amyloid precursor protein. *Nature, 391,* 387-390.

Diebel, M.A., Ehmann, W.D., & Markesberry W.R. (1996). Copper, iron and zinc imbalances in severely degenerated brain regions in Alzheimer's disease: possible relation to oxidative stress. *Journal of Neurological Sciences, 143,* 137-142.

Evin, G. & Weidemann, A. (2002). Biogenesis and metabolism of Alzheimer's disease Aβ amyloid peptides. *Peptides, 23,* 1285-1297.

Falangola, M.F., Lee, S.P., Nixon, R.A., Duff, K., & Helpern, J.A. (2005). Histological co-localization of iron in Aβ plaques in PS/APP transgenic mice. *Neurochemical Research, 30(2),* 201-205.

Farrer, L.A., Cupples, L.A., Haines, J.L., Hyman, B., Kukull, W.A., Maueux, R., & Myers, R.H. et al. (1997). Effects of age, sex, and ethnicity of the association between apolipoprotein E genotype and Alzheimer's disease. A meta-analysis. APOE and Alzheimer Disease Meta Analysis Consortium. *Journal of the American Medical Association, 278(16),* 1349-1356.

Frederickson, C.J., Koh, J.Y., & Bush, A.I. (2005). The neurobiology of zinc in health and disease. *Nature Reviews Neuroscience, 6,* 449-462.

Glenner, G.G. & Wong, C.W. (1984). Alzheimer's disease: initial report of the purification and characterization of a novel cerebrovascular amyloid protein. *Biochemical and Biophysical Research Communications, 120(3),* 885-890.

Haass, C. & Selkoe, D. J. (2007). Soluble protein oligomers in neurodegeneration: lessons from the Alzheimer's amyloid β-peptide. *Nature Reviews Molecular Cell Biology, 8,* 101-112.

Hardy, J. & Selkoe, D.J. (2002). The amyloid hypothesis of Alzheimer's disease: Progress and problems on the road to therapeutics. *Science, 297,* 353-356.

Harris, F.M., Brecht, W.J., Xu, Q., Tesseur, I., Kekonious, L., Wyss-Coray, T., & Fish, J.D. et al. (2003). Carboxyl-terminal-truncated apolipoprotein E4 causes Alzheimer's disease-like neurodegeneration and behavioral deficits in transgenic mice. *Proceedings of the National Academy of Science U.S.A., 100(19),* 10966-10971.

Hill, J. A. (1988). The distribution of iron in the brain. in Youdim, M. B. H. (Ed.), *Brain iron: Neuro- chemistry and behavioural aspects*.(1-24). London: Taylor & Francis.

Hsiao, K., Chapman, P., Nilsen, S., Eckman, C., Harigaya, Y., Younkin, S. & Yang, F. et al. (1996). Correlative memory deficits, aβ elevation, and amyloid plaques in transgenic mice. *Science, 274,* 99-102.

Huang, X., Atwood, C.S., Moir, R.D., Hartshom, M.A., Vonsattel, J.P., Tanzi, R.E., & Bush, A.I. (1997). Zinc-induced Alzheimer's Abeta1-40 aggregation is mediated by conformational factors. *Journal of Biological Chemistry, 272,* 26464-26470.

Huang, X., Cuajungco, M.P., Atwood, C.S., Hartshorn, M.A., Tyndall, J.D., Hanson, G.R. & Stokes K.C. et al. (1999). Cu(II) potentiation of alzheimer abeta neurotoxicity. Correlation with cell-free hydrogen peroxide production and metal reduction. *Journal of Biological Chemistry, 274(52),* 37111-37116.

Hung, Y.H., Bush, A.I., & Cherny, R.A. (2010) Copper in the brain and Alzheimer's disease. *Journal of Biological Inorganic Chemistry, 15,* 61-76.

Janus, C., Chishti, M.A., & Westaway, D. (2000). Transgenic mouse models of Alzheimer's disease. *Biochemica et Biophysica Acta, 1502(1)*, 63-75.

Jones, K.W., Gordon, B.M., Hanson, A.L., Kwiatek, W.M., & Pounds, J.G. (1988). X-ray fluorescence with synchrotron radiation. *Ultramicroscopy, 24*, 313-328.

Klunk, W.E., Engler, H., Nordberg, A., Wang, Y., Blomqvist, G., Holt, D., & Bergstrom, M. et al. (2004). Imaging brain amyloid in Alzheimer's disease with Pittsburgh compound-b. *Annals of Neurology, 55(3),* 306-319.

Kobayashi, D.T., & Chen, K.S. (2005). Behavioral phenotypes of amyloid-based genetically modified mouse models of Alzheimer's disease. *Genes, Brain, and Behavior, 4(3),* 173-196.

Kowalska, A. (2004). Genetic basis of neurodegeneration in familial Alzheimer's disease. *Polish Journal of Pharmacology, 56,* 171-178.

Kuo, Y.M., Emmerling, M.R., Vigo-Pelfrey, C., Kasunic, T.C., Kirkpatrick, J.B., & Murdoch, G.H. et al. (1996). Water-soluble Aβ (N-40, N-42) oligomers in normal and Alzheimer disease brains. *Journal of Biological Chemistry, 271,* 4077-4081.

Lee, J.Y., Cole, T.B., Palmiter, R.D., Suh, S.W., & Koh, J.Y. (2002). Contribution by synaptic zinc to the gender-disparate plaque formation in human Swedish mutant APP transgenic mice. *Proceedings of the National Academy of Science U.S.A., 99(11),* 7705-7710.

Lovell, M.A., Robertson, J.D., Teesdale, W.J., Campbell, J.L., & Markesbery, W.R. (1998). Copper, iron, and zinc in Alzheimer's disease senile plaques. *Journal of Neurological Sciences, 158,* 47-52.

Lue, L.F., Kuo, Y.M., Roher, A.E., Brachova, L., Shen, Y., Sue, L., Beach, T., & Kurth, J.H. et al. (1999). Soluble amyloid β peptide concentration as a predictor of synaptic change in Alzheimer's disease. *American Journal of Pathology, 155(3),* 853-862.

Mathie, A., Sutton, G.L., Clarke, C.E., & Veale, E.L. (2006). Zinc and copper: Pharmacological probes and endogenous modulators of neuronal excitability. *Pharmacology & Therapeutics, 111,* 567-583.

Maynard, C.J., Bush, A.I., Masters, C.L., Cappai, R., & Li, Q. (2005). Metals and amyloid-β in Alzheimer's disease. *International Journal of Experimental Pathology, 86,* 147-159.

Maynard, C.J., Cappai, R., Volitakis, I., Cherny, R.A., White, A.R., Beyreuther, K., & Masters, C.L. et al. (2002). Overexpression of Alzheimer's disease amyloid-beta opposes the age-dependent elevations of brain copper and iron. *Journal of Biological Chemistry, 277,* 44670-44676.

McCall, K.A., Huang, C., & Fierke, C.A. (2000). Function and mechanism of zinc metalloenzymes. *Journal of Nutrition, 130,* 1437-1446.

Miller, L.M., Ruppel, M.E., Ott, C.H., Smith, R.J., & Lanzirotti, A. (2005). Development and applications of an epifluorescence module for synchrotron X-ray fluorescence microprobe imaging. *Review of Scientific Instruments, 76,* 066107.

Mocchegiani, E., Bertoni-Freddari, C., Marcellini, F., & Malavolta, M. (2005). Brain, aging, and neurodegeneration: role of zinc ion availability. *Progress in Neurobiology, 75,* 367-390.

Moos, T., Rosengren, N.T., Skjorringe, T., & Morgan, E.H. (2007). Iron trafficking inside the brain. *Journal of Neurochemistry, 103(5),* 1730-1740.

Moir, R.D., Atwood, C.S., Romano, D.M., Laurans, M.H., Huang, X., Bush, A.I. & Smith, J.D. et al. (1999). Differential effects of apolipoprotein E isoforms on metal-induced aggregation of Aβ using physiological concentrations. *Biochemistry, 38,* 4595-4603.

Naslund, J., Haroutunian, V., Mohs, R., Davis, K.L., Davies, P., Greengard, P., & Buxbaum, J.D. (2000). Correlation between elevated levels of amyloid β-peptide in the brain and cognitive decline. *Journal of the American Medical Association, 283,* 1571-1577.

Newman, M., Musgrave, F.I., & Lardelli, M. (2007). Alzheimer's disease: Amyloidogenesis, the presenilins, and animal models. *Biochimica et Biophysica Acta, 1772,* 285-297.

Nunomura, A., Perry, G., Aliev, G., Hirai, K., Takeda, A., Balraj, E.K., & Jones, P.K. et al. (2001). Oxidative damage is the earliest event in Alzheimer's disease. *Journal of Neuropathology & Experimental Neurology, 60,* 759-767.

Opazo, C., Huang, X., Cherny, R.A., Moir, R.D., Roher, A.E., &White, A.R. et al. (2002). Metalloenzyme-like activity of Alzheimer's disease beta-amyloid. Cu-dependent catalytic coversion of dopamine, cholesterol, and biological reducing agents to neurtoxic H(2)O(2). *Journal of Biological Chemistry, 277,* 40302-40308.

Paxinos, G. & Franklin, K.B.J. (2008). *The Mouse Brain in Stereotaxic Coordinates,* 3rd Ed. New York: Elsevier.

Ramassamy, C., Averill, D., Beffert, U., Bastianetto, S., Theroux, L., & Lussier-Cacan, S. et al. (1999). Oxidative damage and protection by antioxidants in the front cortex of Alzheimer's disease is related to the apolipoprotein E genotype. *Free Radical of Biology and Medicine, 27,* 544-553.

Raux, G., Guyant-Marechal, L., Martin, C., Bou, J., Penet, C., Brice, A., & Hannequin, D. et al. (2005). Molecular diagnosis of autosomal dominant early onset Alzheimer's disease: an update. *Journal of Medical Genetics, 42,* 793-795.

Salminen, A., Ojala, J., Suuronen, T., Kaarniranta, K., & Kauppinen, A. (2008). Amyloid-beta oligomers set fire to inflammasomes and induce Alzheimer's pathology. *Journal of Cellular and Molecular Medicine, 12 (6a),* 2255-2262.

Sambamurti, K., Hardy, J., Refolo L.M., & Lahiri, D.K. (2002). Targeting APP metabolism for the treatment of Alzheimer's disease. *Drug Development Research, 56 (2),* 211-227.

Sayre, L.M., Perry, G., Harris, P.L., Liu, Y., Schubert, K.A., & Smith, K.A. (2000). In Situ oxidative catalysis by neurofibrillary tangles and senile plaques in Alzheimer's Disease. *Journal of Neurochemistry, 74(1),* 270-279.

Scheuner, D., Eckman, C., Jensen, M., Song, X., Citron, N., Suzuki, T.D., & Bird J. et al. (1996). Secreted amyloid beta-protein similar to that in senile plaques of Alzheimer's disease is increased in vivo by the presenilin 1 and 2 and APP mutations linked to familial Alzheimer's disease. *Nature Medicine, 2,* 864-870.

Schipper, H.M. (2009). Apolipoprotein E: Implications for AD neurobiology, epidemiology, and risk assessment. *Neurobiology of Aging, Epublication.*

Seshadri, S., Drachman, D.A., & Lippa, C.F. (1995). Apolipoprotein E epsilon 4 allele and the lifetime risk of Alzheimer's disease. What physicians know, and what they should know. *Archives of Neurology, 52(11),* 1074-1079.

Selkoe, D. (1998). The cell biology of β-amyloid precursor protein and presenilin in Alzheimer's disease. *Trends in Cell Biology, 8,* 447-453.

Shen J. & Kelleher R.J. (2007). The presenilin hypothesis of Alzheimer's disease: Evidence of loss-of-function pathogenic mechanism. *Proceedings of the National Academy of Science, 104(2),* 403-409.

Smith, D.G., Cappai, R., & Barnham, K.J. (2007). The redox chemistry of the Alzheimer's disease amyloid β peptide. *Biochemica et Biophysica Acta, 1768,* 1976-1990.

Smith, M.A., Wehr, K., Harris, P.L., Siedlak, S.L., Connor, J.R., & Perry, G. (1998). Abnormal localization of iron regulatory protein in Alzheimer's disease. *Brain Research, 788,* 232-236.

Squire, L.R. (1992). Memory and the hippocampus: a synthesis of findings with rats, monkeys, and humans. *Psychological Review, 99(2),* 195-231.

Sulwalsky, M., Villena, F., Cardenas, H., Norris, B., Sotomayor, C.P., & Zatta, Paolo. (2003). Cupric and mercuric ions affect the structure and functions of cell membranes. In Paolo Zatta (Ed.), *Metal Ions and Neurodegenerative Disorders,* (427-439), London: World Scientific Publishing Co. Pte. Ltd.

Tanzi, R.E., Gusella J.F., Walkins, P.C., Bruns, G.A., St. George-Hyslop, P., Van Keuren, M.L., Patterson, D., Pagan, S., Kurnit, D.M., & Neve, R.L. (1987). Amyloid beta protein gene: cDNA, mRNA distribution, and genetic linkage the Alzheimer locus. *Science, 235,* 880-884.

The Universal Protein Resource (UniProt) in 2010

Nucleic Acids Res. 38:D142-D148 (2010).

Tsai, J., Grutzendler, J., Duff, K., & Gan, W.B. (2004). Fibrillar amyloid deposition leads to local synaptic abnormalities and breakage of neuronal branches. *Nature Neuroscience, 7,* 1181-1183.

White, A.R., Reyes, R., Mercer, J.F., Camakaris, J., Zheng, H., Bush, A.I. & Multhaup, G. et al. (1999). Copper levels are increased in the cerebral cortex and liver of APP and APLP2 knockout mice. *Brain Research, 842,* 439-444.

Wilcock, D.M., Vitek, M.P., & Colton, C.A. (2009). Vascular amyloid alters astrocytic water and potassium channels in mouse models and humans with Alzheimer's disease. *Journal of Neuroscience, 159(3),* 1055-1069.

Curriculum Vitae

Erinn S. Gideons graduated from the Governor's School for Government and International Studies at Thomas Jefferson High School, Richmond, Virginia, in 2001. She received her Bachelor of Arts, cum laude, in Psychology from University of North Carolina in 2005. She was in the Intramural Training Research Award Program at the National Institutes of Health from 2008-2010. Erinn received her Master of Arts in Psychology with a concentration in Biopsychology from George Mason University in 2010.